Title
Rainfall-runoff response following the 2010 Bull Fire in southern Sequoia National Forest, California

Author
Hale, Brandon

Publication Date
2012

Peer reviewed|Thesis/dissertation

UNIVERSITY OF CALIFORNIA

Los Angeles

Rainfall-runoff response following the 2010 Bull Fire in southern Sequoia National Forest, California

A thesis submitted in partial satisfaction

of the requirements for the degree of Master of Science

in Civil Engineering

by

Brandon Charles Hale

2012

ABSTRACT OF THE THESIS

Rainfall-runoff response following the 2010 Bull Fire in southern Sequoia National Forest, California

by

Brandon Charles Hale

Master of Science in Civil Engineering

University of California, Los Angeles, 2012

Professor Terri S. Hogue, Co-chair

Professor Steven Margulis, Co-chair

Wildfires alter land surfaces and land-atmosphere interactions, causing enhanced runoff and debris flows. The current study evaluates hydrologic behavior and recovery for three watersheds in the burned in the 2010 Bull Fire in the southern Sequoia National Forest. One unburned watershed was selected outside the fire perimeter for a control. The effects of wildfires have been extensively analyzed, but these studies typically focus on debris flows immediately following the fire and vegetation recovery on a plot-scale. This study attempts to evaluate hydrologic recovery through in-situ instruments in areas analyzed by a United States Forest Service Burned Area Emergency Response team. Many agencies attempt to predict post-fire

runoff peaks and volumes to identify values-at-risk and determine if protective measures must be implemented. The four study sites are instrumented with tipping buckets and pressure transducers to measure precipitation and discharge throughout the approximate two year study period. Stream discharge is measured at five-minute intervals, the tipping buckets are event-based to track storm duration and intensity, and channel cross-sections are measured every two months to detail sediment deposition or scour that accompany rainfall-runoff events. Precipitation was found to be consistent between the study areas, but a link between precipitation and cross-section area changes was not determined. Geomorphic parameters were evaluated with an area-normalized discharge to determine correlations. Aspect, soil type, and watershed shape were found to be the controlling factors in elevated discharge. To judge watershed recovery, the response lag, lag-to-peak, and runoff ratio were calculated for 13 selected storms across all study sites. Variability of each parameter was determined to depend on the precipitation tipping bucket location and the time between storms. Recovery was unable to be determined based on the three rainfall-runoff hydrograph parameters. Future work involves relating a remote sensing vegetation index with the storm parameters to couple vegetation recovery with hydrologic recovery and gain insight into watershed recovery on a storm-by-storm basis.

The thesis of Brandon Charles Hale is approved.

William W-G. Yeh

Jennifer A. Jay

Steven Margulis, Committee Co-chair

Terri S. Hogue, Committee Co-chair

University of California, Los Angeles

2012

Table of Contents

Acknowledgements

This report would not have been possible without help from a multitude of kindhearted people. I would like begin by thanking Dr. Terri Hogue for her guidance and mentorship. Next, a special thank you goes to Dr. Alicia Kinoshita for her constant feedback and assistance. A large thanks is owed to Carolyn Napper of the U.S. Forest Service for the vision and resources she provided. Additionally, field work for the past two years required the helping hands of many. Field days often required trekking miles uphill, in sweltering heat or bone-chilling snow, while avoiding rattlesnakes hiding beneath rocks. The work was not for the faint of heart, but was always rewarded with tasty tacos from El Rio in Kernville, CA. I am very grateful for the field help provided by:

- UCLA Fire Team: Alicia Kinoshita, Tristan Acob, Sharon Liu, Laura McNerney, Karen Chu, and Bryant Reyes
- U.S. Forest Service: Christopher Stewart, Marc Stamer, Kevin Cooper, and the U.S.F.S. Kernville office
- Cal Tech: Steve Skinner

Furthermore, this project was funded by the U.S.D.A./U.S.F.S. grant #1113810020 and N.S.F. Hydrologic Sciences E.A.R. #0965236. Finally, I would like to thank my committee for graciously donating their time to review this report: Terri Hogue, Steve Margulis, William Yeh, and Jenny Jay. I am very appreciative for everyone who has helped me complete this milestone in my life.

Introduction

Climate warming, anthropological impacts, and forest management have led to an increase in wildfire occurrence, size, and severity in the Southwestern United States (Baker, 1993; Keeley et. al., 1999; Westerling et. al., 2006; Running, 2006; Kitzberger et. al., 2007; Pechony and Shindell, 2010). The Earth's surface temperature has increased an average of 0.87 degrees Celsius from 1987 to 2003 (Westerling et. al., 2006). This temperature increase contributes to earlier snowmelt and drier vegetation (Running, 2006). Dried vegetation provides higher fuel levels for fires, resulting in larger fires that burn hotter and more aggressively (Kauffman, 2004). Additionally, throughout the majority of the twentieth century, forest managers followed the policy of immediate wildfire suppression, which prevented regular burns across large areas to reduce fuel loads (Baker, 1993; Keeley et. al., 1999; Ice et. al., 2004). Furthermore, the increase in human population has resulted in an increase in the number of human ignited wildfires over the past 30 years (Keeley et. al., 1999; Radeloff et. al., 2005; Westerling et. al., 2006). In the 2000 wildfire season, 43% of the wildfires in the United States were human ignited (Radeloff et. al., 2005).

Wildfires can be devastating to local ecosystems in the short term, resulting in the loss of vegetation and plant interception, increased erosion rates, deterioration of water quality, and a temporary hydrophobic top-soil layer (DeBano, 2000; Moody and Martin, 2001; Jung et. at., 2009; Burke et. al., 2010; Kinoshita and Hogue, 2011; Ebel et. al., 2012). These factors combine to produce an unstable top soil layer that can become mobilized during precipitation events (Scott, 1971; Wells, 1981; Wells, 1987). In 2003, more than 4,220 homes were destroyed, and the majority of those were in southern California (Radeloff et. al., 2005). That same year, 16

people died during a massive debris flow downstream of the Old Fire in San Bernardino, California (Chong et. al., 2004). These severe consequences following wildfires have garnered attention from researchers and the public, and the changes to the burned watersheds and post-fire processes are of great concern to downstream communities.

Depending on the soil burn severity, the soil undergoes changes in physical and chemical processes (DeBano, 2000; Moody et. al., 2008). When decaying debris above the soil surface burns hot enough, the organic material in the top-soil volatizes during oxidation, and upon cooling the volatized organic compounds creates a negatively charged hydrophobic layer (Savage, 1974; DeBano, 2000; Letey, 2001; Ice et. al., 2004). The hydrophobic top-soil layer decreases infiltration and increases overland flow, resulting in dramatically increased post-fire runoff levels (Krammes and DeBano, 1965). The effects of wind, rain splash, and overland flow erode the hydrophobic layer over time (Terry and Shakesby, 1993; Martin and Moody, 2001). Without the hydrophobic layer, the top soil becomes vulnerable to precipitation and water flow. Storm events can mobilize instable soil by overland flow, and along with litter from the fire, produce large debris flows (Kutiel et. al., 1995). Studies frequently focus on understanding debris flows and attempting to predict their occurrence (Gabet, 2003; Fox et. al., 2007; Shakesby, 2011) because of devastating impacts downstream.

Identifying when a watershed recovers is important for structures and lives threated by elevated discharge and debris flows. Hydrologic recovery varies between watersheds and is based on the number of storm events, vegetation regrowth, burn severity, and geomorphic parameters such as slope, aspect, and soil type (Fox et. al., 2006; Shakesby, 2011; Kinoshita and Hogue, 2011). Recovery of discharge to pre-fire levels can take many years. Vegetation is vital

in watershed recovery due to its role in precipitation interception and water uptake, reducing discharge downstream. The amount of vegetation remaining after a fire is dependent on the burn severity. Burn severity is a variable of post-fire runoff rates because the removal of the canopy layer, which intercepts rainfall, increases discharge downstream (Zinke, 1967). Removal of the understory canopy, duff, and litter eliminates obstructions, resulting in quick rainfall-runoff responses and higher peak discharges (Gilley et. al., 1992). Vegetation regrowth can occur within a few months for grassland, but recovery of pre-fire land cover can take years depending on controlling parameters (Kinoshita and Hogue, 2011). Locations of low severity burns with north and east aspects show highest recovery rates, likely due to retained soil moisture (Casady et. al., 2009; Kinoshita and Hogue, 2011). High burn severity locations have the longest recovery times due to larger initial loss in biomass and precursors to vegetation regrowth, such as root structure and seed availability (Kinoshita and Hogue, 2011). Understanding recovery and how it is linked to burn severity and geomorphic parameters is important in evaluating downstream values-at-risk to elevated runoff.

To mitigate the impact of post-fire hydrologic response to lives, structures, and natural resources downstream of burned watersheds, the United States Forest Service (USFS) has tasked their Burned Area Emergency Response (BAER) teams with the responsibility of identifying values-at-risk and prescribing emergency treatments (Witt, 1999; Stewart and Kaplan-Henry, 2010). It is vital to accurately predict the post-fire rainfall-runoff response to guide management decisions. Particular interest is paid to peak discharge, as structures downstream must be capable withstanding this maximum discharge. In the last decade, researchers have developed threshold and physically-based peak flow and debris flow models (Wilson et. al., 2001; Rulli and Rosso,

2007; Cydzik and Hogue, 2009). To enhance post-fire management, accurate model prediction is necessary for proper allocation of limited resources, evaluation of watershed recovery, and improved understanding of watershed-scale rainfall-runoff response.

Previous studies have analyzed the post-fire rainfall-runoff response on the plot scale (Moody et. al., 2008) and the basin scale (Kinoshita and Hogue, 2011). Moody et. al. (2008) developed a linear relationship between rainfall and discharge, using the Rational Method, for four watersheds roughly the size of 0.28 square kilometers in Rendija Canyon, New Mexico. Rainfall-runoff response was determined to be dependent on the rainfall intensity and not the burn severity. However, the analysis performed compared instantaneous discharge measurements with a 30-minute time averaged rainfall amount, eliminating the potential for storm analysis. Kinoshita and Hogue (2011) analyzed the rainfall-runoff response at a basin level to compare watershed recovery with remotely sense vegetation indices. Two southern California basins were studied, Devil Canyon and City Creek, 14.2 and 50.8 square kilometers respectively. Kinoshita and Hogue (2011) concluded that overall discharge levels were still elevated after seven years due to steep slopes and slow vegetation recovery in higher elevations, higher burn severity areas, and south and west aspects. Neither study analyzed watershed behavior on a storm event basis. The current study analyzes the 2010 Bull Fire, which occurred in the Southern Sequoia National forest in Tulare County, California. Three sites were instrumented within the fire perimeter (Bull 1, 2, and 3) and an unburned control site (Bull Control) was established outside the fire perimeters, with five-minute resolution observations to monitor post-fire rainfall-runoff for approximately two years. Storms were selected and analyzed to monitor the hydrologic recovery.

The goals of this study are:

1. Analyze the post-fire rainfall-runoff response and relate to geophysical (aspect, slope, elevation) parameters, pre-fire vegetation, and climate properties at the 2.5-4.4 square kilometer watershed size

2. Quantify post-fire storm rainfall-runoff response (lag time, time-to-peak, runoff ratio) to analyze and evaluate recovery trends

3. Establish a relationship between frequent cross-section measurements at study site outlets (proxy of sediment deposition or scour) to storm events, slope, and soil type to understand sediment fluxes in the contributing area.

Study Area

The Bull Fire occurred in the Southern Sequoia National Forest, north of Kernville, CA. Approximately 66.5 square kilometers burned between July 26, 2010 and August 10, 2010. Post-fire concerns included downstream infrastructure such as Kernville and Isabella Lake reservoir. The USFS Remote Sensing Applications Center (USFS RSAC) Burned Area Reflectance Classification (BARC) map (Figure 1) provides soil burn severity estimates for the Bull Fire (USFS RSAC, 2010).

Three study sites (Bull 1, Bull 2, and Bull 3) were established within the fire perimeter (Figure 1). Locations of these sites were selected due to their coupled aspects (Table 1), largely moderate burn severity (Table 2), and ease of access. All sites were carefully installed to ensure they were removed from public access, eliminating human interference. Bull 1 is a contributing area to Bull 2, which was chosen to allow for the partitioning of flow within the watershed to evaluate controlling discharge parameters. Bull 1 and Bull 2 both have generally westward aspects, while Bull 3 was chosen due to its general eastward aspect (Table 1). An unburned site, Bull Control, was established four kilometers north of the fire perimeter (Figure 1) to allow for comparisons between the burned sites. Bull Control has a general westward aspect.

The California Department of Water Resources estimates the average annual precipitation for the Kernville area to be 47 centimeters (CA DWR CDEC, 2012). The precipitation data is measured at the Kern River Power House Intake Number 3, approximately ten kilometers north of the burn perimeter at an elevation of 1,113 meters. The majority of precipitation occurs during the winter season with rainfall as the primary precipitation, but snow possible at upper

elevations. Of the study sites, Bull 2 has the lowest outlet elevation at 924 meters and Bull Control has the highest top elevation at 2,606 meters (Table 1). During our study period, the 2011 water year (WY) was wetter than average with approximately 70 centimeters and the 2012 water year was drier than average with approximately 25 centimeters of rainfall at the study sites. While neither year is considered an El Nino or La Nina occurrence, this climatology will affect watershed recovery.

Table 1: Geomorphic parameters (USGS NED, 2002)

Parameter	Bull 1	Bull 2	Bull 3	Bull Control
Outlet Latitude (°)	35.84	35.84	35.83	35.89
Outlet Longitude (°)	-118.44	-118.45	-118.46	-118.46
Area (km^2)	2.56	4.4	4.14	4.17
Outlet Elev. (m)	1,074	924	947	1,042
Top Elev. (m)	1,946	1,946	2,083	2,606
Reach Length (m)	2,317	3,637	4,088	4,410
Watershed Length (m)	2,464	3,955	4,651	4,859
Slope (%)	35	26	24	32
Soil Type*	C	C	D	D

* NRCS, 2012

Table 2: Burn severity (USFS RSAC, 2010)

Burn Severity	Overall	Study Sites		
		Bull 1	Bull 2	Bull 3
Unburned	8%	6%	10%	16%
Low	33%	14%	13%	13%
Moderate	58%	79%	77%	68%
High	1%	1%	0%	3%

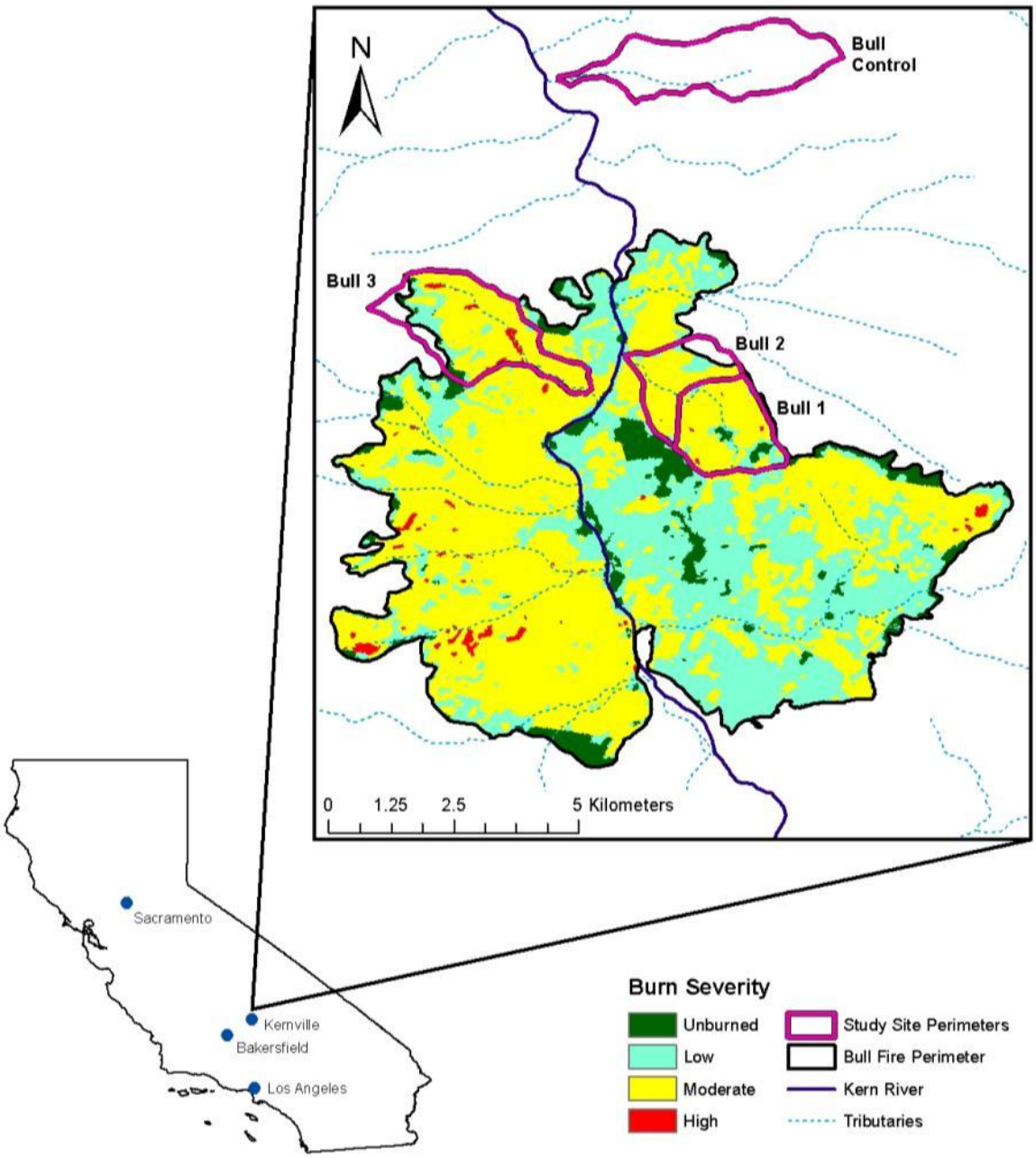

Figure 1: Bull Fire perimeter with burn severity (USFS RSAC, 2010) and study sites

The last major fire in the area that completely burned our study sites occurred in 1942 (FRAP, 2012) and minor wildfires that have burned within the Bull Fire 2010 perimeter occurred in 1964, 1969, 1983, 2003, and 2009. The 2009 Corral fire partially burned Bull 2 with mostly low soil burn severity, while the remaining fires did not affect our specific study sites (FRAP, 2012). In 2007, the Goldledge fire burned approximately two-thirds of the Bull Control area (FRAP, 2012) but the watershed visually appeared recovered at the time of installation in 2010.

Geomorphic parameters (Table 1) for the study areas affect rainfall-runoff response. Watershed parameters were calculated from the USGS National Elevation Dataset (NED) at a 30 meter by 30 meter resolution. Watershed slopes range from 24 to 35%, with Bull 1 and Bull Control greater than 30%. With the exception of Bull 1, which is a contributing area to Bull 2, all sites are similar in size. Soil type, developed by a weighted average from the NRCS Web Soil Survey (WSS), yielded type C for Bull 1 and Bull 2, and type D for Bull 3 and Bull Control (Table 1). Type C soils are clay loams that are low in organic content; type D soils are heavy plastic clays that swell significantly when wet (Mays, 2001).

Pre-fire land cover was predominantly shrubland (Table 3), though forest is present at higher elevations. Herbaceous vegetation is generally low, except in Bull 3, where flow is perennial. Spatial variation of pre-fire land cover at each site is in Appendix A.

Table 3: Land cover (USGS NLCD, 2006)

Land Cover (%)	Bull 1	Bull 2	Bull 3	Bull Control
Forest	19%	16%	16%	44%
Shrubland	79%	78%	68%	53%
Herbaceous	2%	6%	17%	3%

Predominant aspect varies by site (Appendix B). Percentage breakdown (Table 4) shows that each study site has two predominant aspects. Each cardinal direction aspect is represented as a predominant aspect in at least one study site.

Table 4: Aspect (USGS NED, 2002)

Aspect	Bull 1	Bull 2	Bull 3	Bull Control
North	36%	37%	17%	11%
East	15%	9%	43%	1%
South	8%	15%	36%	51%
West	42%	38%	4%	38%

Methods

In Situ Observations

Channel Cross-Sections

Cross-section selection at each site was determined based on various factors. The cross-sections minimized hydraulic jump to reduce water stage height uncertainties. The channel was relatively straight with no overhanging rocks and the cross-section was not immediately downstream of turbulent flows. Edges of the cross-section were permanently established with rebar or by utilizing boulders or trees. This allowed for consistent cross-section measurements with an optical bench level for each site visit (Table 5). A tape measure guided vertical measurements, typically every 0.3 to 0.6 meters along the edges of the channel and 0.15 meters along the streambed to better capture channel changes. The ends of each cross-section were measured to allow for comparisons between visits through a common point to evaluate the change in area.

Table 5: Visit date for each cross-section

Visit Number	Bull 1	Bull 2	Bull 3	Bull Control
1	09/20/2010	09/20/2010	10/29/2010	11/29/2010
2	10/13/2010	10/13/2010	11/29/2010	01/22/2011
3	11/29/2010	11/28/2010	01/22/2011	03/15/2011
4	01/22/2011	01/22/2011	03/15/2011	04/30/2011
5	03/14/2011	03/15/2011	04/29/2011	06/30/2011
6	04/29/2011	04/29/2011	07/01/2011	
7	06/30/2011	06/29/2011	08/18/2011	
8	08/18/2011	08/17/2011	10/20/2011	
9	10/21/2011	10/20/2011	12/11/2011	
10	12/11/2011	12/10/2011	02/04/2012	
11	02/04/2012	02/03/2012	04/07/2012	
12	04/07/2012	04/07/2012	06/12/2012	
13	06/12/2012	06/12/2012	10/12/2012	
14	10/12/2012	10/12/2012		

Site Instrumentation

Each study site was instrumented with a pressure transducer and a tipping bucket (Appendix B). The pressure transducer (Onset HOBO U20-001-01) recorded at a five minute interval, allowing for a 56-day deployment until the data had to be downloaded and the device re-launched. The HOBO house was placed immediately above the channel surface and attached to a fence post with zip-ties (Figure 2). Refer to Appendix C for HOBO deployment methodology. With each visit, the HOBO's vertical location was adjusted up or down, depending on channel scour or deposition, to ensure the device was always resting on top of the channel bed. HOBO installation dates varied between September to November, 2010 (Table 6). Bull

Control experienced an intense and localized thunderstorm on July 30, 2010, which yielded high water flow and debris flow that washed out the channel HOBO. All other sites were uninstalled on August 26, 2012.

Figure 2: HOBO house deployed (Bull Control)

The Onset HOBO pressure transducer measures absolute pressure. To parse out atmospheric pressure, a HOBO was installed on a nearby channel bank, known as an air HOBO. To compensate for missing data at the beginning of the project, a linear relationship was established between the air HOBO at Bull 2 with Bull 1 and Bull Control for the periods where both devices were operating. The relationship between Bull 1 and Bull 2 was developed through 79,950 common measurements and between Bull Control and Bull 2 through 95,632 common measurements (Appendix D). Rainwise precipitation tipping buckets were installed throughout the study areas. Bull 1 and Bull 2 share the same tipping bucket (Bull 1). The tipping buckets

recoded the date and time of each tip, where a tip represents 0.01 cm of precipitation. Utilizing a MATLAB script, the tips were truncated to the nearest minute and then aggregated to a five minute time interval to match the HOBO timeseries.

Table 6: Site instrumentation installation and uninstallation dates

Location		Channel HOBO	Air HOBO	Tipping Bucket
Bull 1	Installation	09/20/2010	06/30/2011*	09/20/2010
	Uninstallation	08/26/2012	08/26/2012	08/26/2012
Bull 2	Installation	09/20/2010	09/20/2010	09/20/2010
	Uninstallation	08/26/2012	08/26/2012	08/26/2012
Bull 3	Installation	10/29/2010	N/A	10/29/2010
	Uninstallation	08/26/2012	N/A	08/26/2012
Bull Control	Installation	11/05/2010	06/30/2011*	11/05/2010
	Uninstallation	06/30/2011	08/26/2011	08/26/2012

* Data linearly interpolated with Bull 2 air HOBO to provide complete data series to the installation date of the channel HOBO

Data Analysis

Conversion of HOBO absolute pressure to discharge

The atmospheric pressure measured by the air HOBO was subtracted from the absolute pressure of the channel HOBO, to provide water pressure. Using the atmospherically corrected pressure, initial height of water above the HOBO, and the HOBOware Pro software, the pressure was converted to stage height by computing a temperature and density corrected depth array using a constant assumed fluid density. Note that the fluid density used is for freshwater: 1,000 kg/m^3. Fluid density is converted to a density dependent fluid depth array (Onset, 2008).

To convert the stage height to a discharge, the cross-sections measured at each visit were used to calculate discharge with Manning's equation (Equation 1). The cross-section measured at the time of the device launch was assumed constant during the deployment. A MATLAB script was utilized to calculate Manning's discharge every five minutes using the geomorphic parameters in Table 7. These values were selected for the representation of normal, natural mountain streams with gravel to boulders (Mays, 2001). During site visits, if discharge was present it was measured using a Marsh-McBirney Flow-mate 2000. Three discharge measurements were recorded at Bull 2, six at Bull 3, and two at Bull Control. Rating curves were developed at each site with the discharge measurements (Appendix E). Slope and Manning's n within the model were lowered and raised, respectively, as Manning's equation overestimated observed discharge. Through the calibration process, it was determined that the most representative slope was calculated from the outlet to 0.40 kilometers upstream. While the model still overpredicts discharge, we believe that errors in measuring low velocities results in undervalued measured discharge.

Equation 1: Manning's equation

$$Q = 1/n * A * R^{2/3} * S^{1/2}$$

Q = discharge (m^3/s)

n = Manning's roughness coefficient (-)

A = cross-sectional area (m^2)

R = hydraulic radius [area/wetted perimeter] (m)

S = channel energy slope (m/m)

Table 7: Parameters used in Manning's equation (USGS NED, 2002)

Parameter	Bull 1	Bull 2	Bull 3	Bull Control
Manning's n (-)	0.04	0.05	0.06	0.05
Slope (%)	7.2	6.5	5.2	4.6

The five-minute discharge time series was transformed with the Box-Cox (Equation 2) to expand low flows to visually compare rainfall-runoff. The transformation dependent variable, λ, can vary between 0 for a log transformation to 1 for no transformation (Box-Cox, 1964). A λ value of 0.3 was selected (Hogue et. al., 2000).

Equation 2: Transformed flow for plotting (Box-Cox, 1964)

$Q_{transform} = ((Q+1)^{\wedge}(\lambda -1))/\lambda$

$Q_{transform}$ = transformed discharge (m^3/s)

Q = original discharge (m^3/s)

λ = transformation variable (-)

Storm Selection

To evaluate the hydrologic recovery of Bull 1, 2, and 3, a total of 13 storms were selected (Table 8), with the majority during water year 2011. The emphasis on storms in WY 2011 were due to 1) a larger selection of storms available, 2) the Bull Control channel HOBO being washed out on July, 2011, and 3) HOBO malfunctions during Spring 2012, resulting in no data.

Table 8: Selected storms for analysis

Storm Number	Storm Begin Date
1	12/17/2010 04:35
2	12/25/2010 19:15
3	12/28/2010 20:10
4	01/30/2011 07:15
5	02/18/2011 18:55
6	02/25/2011 07:35
7	03/18/2011 22:30
8	03/24/2011 19:35
9	04/07/2011 12:55
10	07/04/2011 14:45
11	07/30/2011 17:40
12	01/23/2012 01:55
13	04/12/2012 22:25

From the selected storms, three parameters will be analyzed: lag response, lag-to-peak, and the runoff ratio. The lag response is the length of time from the start of precipitation to the start of the runoff response. The lag-to-peak is the length of time from the start of precipitation to the peak of the runoff response. The runoff ratio is the unit depth of discharge (Equation 3) divided by the unit depth of precipitation.

Equation 3: Conversion of discharge volume to depth

$Q = sec\_to\_min * min\_interval / (A * (mile^2\_to\_ft^2)) * ft\_to\_cm$

sec_to_min = conversion of seconds to minute = 60 sec/min

min_interval = aggregation to 5-minute interval = 5 min

A = watershed area in square miles

$mile^2\_to\_ft^2$ = conversion of square miles to square feet = 5280^2 ft^2

ft_to_cm = conversion of feet to centimeters = 30.48 cm

Results and Discussion

Precipitation Comparison

Precipitation varied at each site (Table 9) due to location, elevation, and aspect. Overall, WY 2011 was a wet year and WY 2012 was a dry year, as the long-term average for the nearby city of Kernville is 47 centimeters. In WY 2011, Bull 1 and Bull 3 received the highest precipitation. In WY 2012, the southern sites received less rainfall and northern sites. The regional gauge at the Kern River Intake #3 reflected similar rainfall patterns as the study sites (Figure 3).

Table 9: Precipitation at study sites and nearby Kern River Intake #3 gauge for water years 2011 and 2012

		Precipitation (cm)	
Location	Elevation (m)	WY 2011	WY 2012
Bull 1	1,074	70	22
Bull 3	918	70	25
Bull Control	1,053	58	26
Kern Intake 3	1,113	65	31

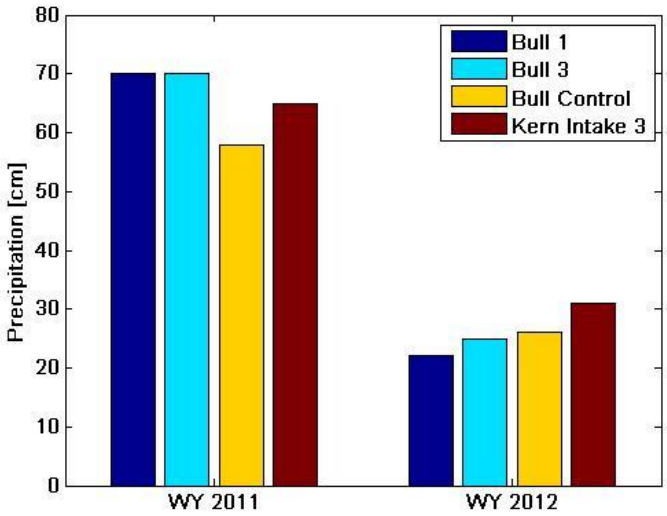

Figure 3: Rainfall for WY 2011 and 2012 at study sites and Kern River Intake #3

A scatter plot analysis is used to understand precipitation variability among sites (Figures 4-6). Since five-minute rainfall data is highly sensitive to instrument location and watershed geomorphic parameters, precipitation data was aggregated to a daily time step. A linear trend line and R-squared value are calculated for each relationship. The correlation is high, with 0.91 between Bull 1 and Bull Control being the lowest. At a daily time step, the sites experienced very similar amounts of rainfall. Overall, Bull 3 received the most rainfall and Bull Control received the least rainfall. Occasionally Bull 1 received less than one centimeter of precipitation while Bull 3 and Bull Control did not (Figures 4 and 5) and Bull Control received more precipitation than Bull 1 and 3 for events ranging from one to four centimeters (Figures 5 and 6). Refer to Appendix F for the entire precipitation timeseries for the three tipping buckets.

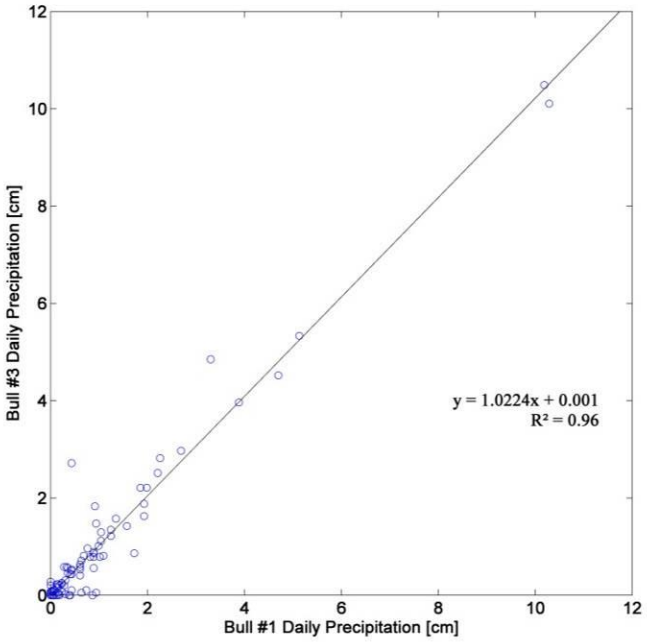

Figure 4: Bull 1 and Bull 3 daily precipitation scatter plot

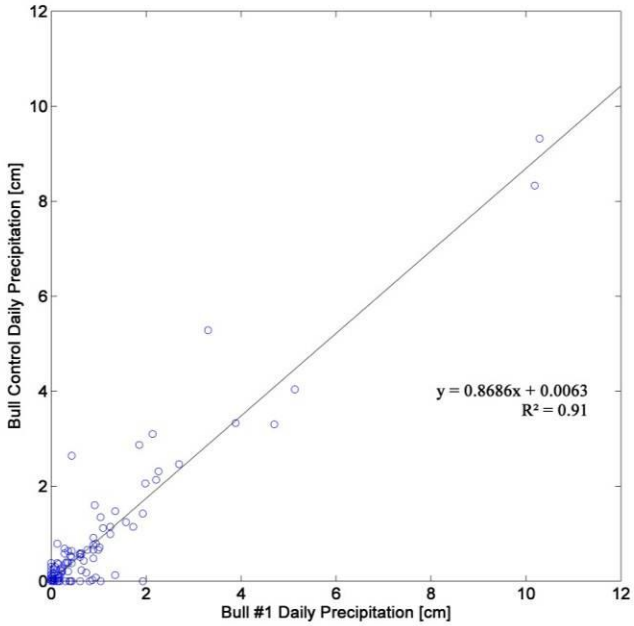

Figure 5: Bull 1 and Bull Control daily precipitation scatter plot

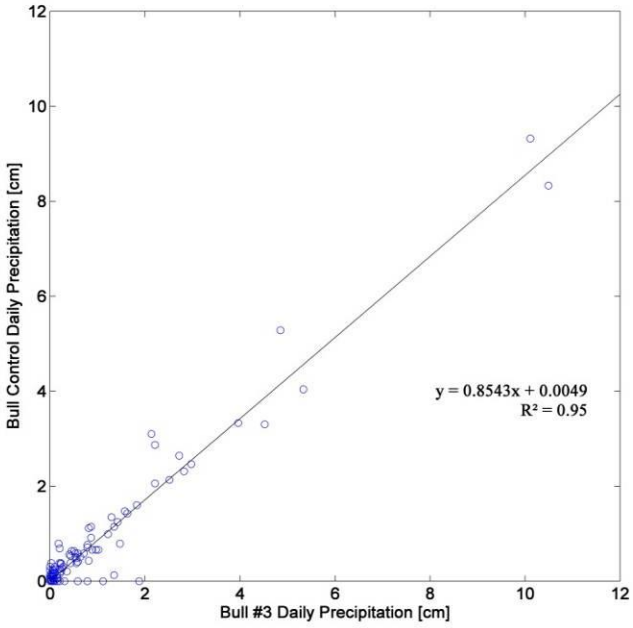

Figure 6: Bull 3 and Bull Control daily precipitation scatter plot

Cross-Section Analysis and Comparisons

Channel cross-sections will naturally change over time. Cross-section measurements made for each visit (Table 5) are in Appendix G. Generally, the largest cross-section changes occurred early in the study period when the top soil was more instable and could easily be mobilized. Sediment was removed at Bull 1, 2, and Control cross-sections between Visit 1 and Visit 2. Sediment was deposited at Bull 3 over the same time period. Factors that influence scour and deposition are the burn severity, soil type, storm intensity, and watershed slope. Bull 3 had more deposition than the other sites due to its low watershed slope (24%) and highest amount of unburned area. Bull Control's cross-section scour can be attributed to its steep slope, at 35

percent. During the remainder of the study period, cross-section change became more subtle. To investigate the relationship between cross-section changes with precipitation, scatter plots of area change between visits versus total precipitation between visits were analyzed (Appendix H); however, no relationship was determined. If cross-section measurements were performed after each storm, rather than every two months, then we expect a relationship between storms and cross-section changes to develop.

Discharge Comparison

If the pressure transducer was buried or suspended in the air between the bimonthly cross-section measurements from deposition or scour, data from that point in time was skewed for the remainder of the time period. This was infrequent and typically at Bull Control due to its gravel streambed. It is possible to estimate when changes to the area surrounding the HOBO occurred, but the data cannot be modified to account for the HOBO location error. Transformed discharge and precipitation timeseries for each site is located in Appendix I. Generally, Bull 3 had the highest discharge response among the sites, especially for the largest precipitation event during the study period occurring on 12/25/2010. Bull 2's storm responses generally followed that of Bull 1, since Bull 1 is a contributing area to Bull 2, but occasionally intense summer storms would incite a high discharge response in one watershed but not in the other. Bull Control had a response pattern similar to Bull 3, but in a smaller magnitude.

To compare discharge between sites, the flow timeseries was normalized by the watershed area (Figure 7). The area-normalized discharge is smaller in Bull 2 than Bull 1

throughout the study period. Bull Control has similar response patterns to Bull 3, which had the highest discharge among the sites. The largest discharge at all sites occurred in December, 2010, which was a response to a high intensity and long duration winter storm.

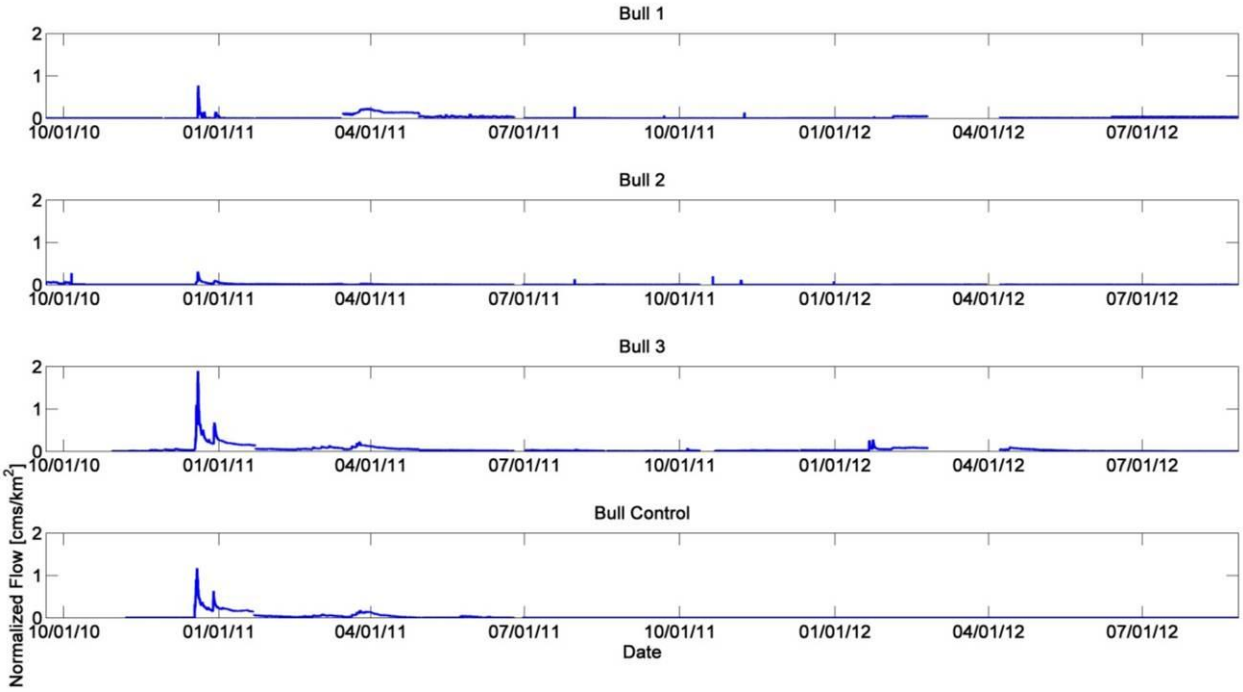

Figure 7: Normalized discharge timeseries

Discharge (Appendix I) variations between the sites arise from differences in watershed slope, aspect, pre-fire vegetation, burn severity, and soil type. In general, steeper watersheds have higher discharge levels due to water's inability to pond. Bull 3 had the highest discharge despite having the lowest watershed slope (24%). Bull 2 and Bull 3 have nearly the same slope, but had very different discharge responses. Bull Control closely followed Bull 3's flow patterns

but to a lesser degree, despite its watershed slope at 32%. While watershed slope is a factor in rainfall-runoff response, it is not the controlling factor.

Aspect (Appendix B) is important in vegetation recovery as each aspect receives varying amounts of solar radiation input. Kinoshita and Hogue (2011) concluded that north aspects recovery more quickly than the other aspects. This study does not currently incorporate vegetation recovery, but solar input affects the soil moisture content, which affects precipitation partitioning. Bull 1 and Bull 2 have the lowest discharge of the study sites and the highest percentage of north aspects at 36% and 37%, respectively. North aspects have lower soil moisture contents, which will allow for more infiltration (assuming similar soil type) and lower runoff. Additionally, south aspects receive the least amount of solar radiation input, so Bull Control (51% south aspect) has the second largest runoff response. This is lower than Bull 3 (36% south aspect), but since Bull Control is unburned and did not have an elevated discharge response, it can be reasonably assumed that southern aspects have higher runoff rates due to higher soil moisture contents. Aspect is a significant factor in rainfall-runoff response.

Pre-fire vegetation is also a significant variable in post-fire rainfall-runoff response. Vegetation with deep root structures, like forest, is more likely to survive low burn severities and continue water uptake in the post-fire environment. Alternatively, shrubland and herbaceous land cover have shallow root structures and burn completely. Pre-fire vegetation was similar among the burn sites (Table 3), with the exception of Bull 3 containing a higher percentage of herbaceous vegetation (17%) than Bull 1 (2%) and Bull 2 (6%). Corresponding, Bull 3 had a lower amount of shrubland, although shrubland was the largest pre-fire vegetation species (68%-79%). Bull Control had a much higher percentage of forest (44%) and a lower shrubland (53%)

when compared to the burn sites. When analyzing the spatial distribution (Appendix A) between the sites, Bull Control has a high amount of forest land in the upper watershed. Bull 1, 2, and 3 had smaller forest amounts (19%, 16%, and 16% respectively), but the forestland in Bull 3 was confined to the south aspect while Bull 1 and Bull 2 had forest throughout the watershed. The similarity of pre-fire land cover in Bull 1, 2, and 3, and the large disparity in runoff response indicate pre-fire land cover does not have a significant impact on the rainfall-runoff response.

Higher burn severities will remove more of the canopy, duff, and litter layers, which enhance overland flow. Refer to Figure 1 for a spatial distribution of burn severities. Bull 3 has the largest percentage of high burn (3%), but also the largest percentage of unburned (16%) among the study sites. The large runoff potential from the high burn is minimized by the large percentage of unburned at Bull 3. Bull 1 has the lowest percentage of unburned (6%), but the largest total burn severity (94%) with the majority moderate (79%); therefore, Bull 1 should experience the highest runoff amount, which did not occur. Overall, burn severity is not the controlling factor in runoff response in the three burned sites.

Other factors that control rainfall-runoff response include soil type and watershed shape. Bull 1 and Bull 2 are predominantly composed of Type C soil with a wide watershed shape, whereas Bull 3 and Bull Control are composed of Type D soil with a narrow watershed. Type D soils have lower infiltration than Type C soil (Mays, 2001), which contributes to Bull 3 and Bull Control experiencing higher runoff. Additionally, the narrow watershed shape lowers the time of concentration, increasing runoff peak and timing. These factors are significant in the rainfall-runoff response in the study sites.

Storm Analysis

To quantify rainfall-runoff response in the study sites, the following variables were calculated for each storm (Appendix J): t_{w0} (beginning of effective water input), t_{we} (end of effective water input), t_{pk} (time of peak discharge), T_W (duration of effective water input), T_{LR} (response lag), T_{LP} (response lag), I (intensity), and RO (runoff ratio). Locations of the tipping buckets minimally affect our data when considered at the daily scale (Figures 4-6). The scatter plots, however, do not reflect variation in elevation, which can be significant when precipitation occurs as rainfall at lower elevations and snowfall at higher elevations. The uncertainty of snowfall at watershed peaks greatly affects rainfall-runoff calculations as runoff can be delayed by snowpack storage. This uncertainty will be reflected in the analysis of the response lag, lag-to-peak, and runoff ratio for each storm.

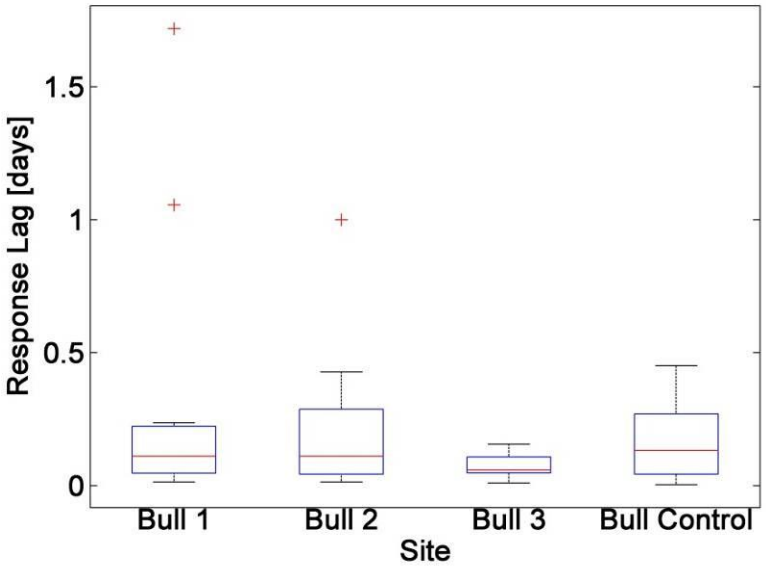

Figure 8: Box plot of response lag for selected storms

Figure 8 shows that Bull 2 and Bull Control have the largest response lag variability. Bull 3 has the lowest variability in response lag due to perennial flow. The perennial flow contributes to higher soil moisture saturation, resulting in a quicker response time as water cannot percolate into the soil. Bull Control has a longer response lag, or at least comparable to Bull 2, because it is unburned. Vegetation understory, duff, and litter layers in Bull Control impede overland flow and lengthen time of concentration. Bull 2 has a similar variability as Bull Control, except Bull 2 has a lower median value (shown as the red line).

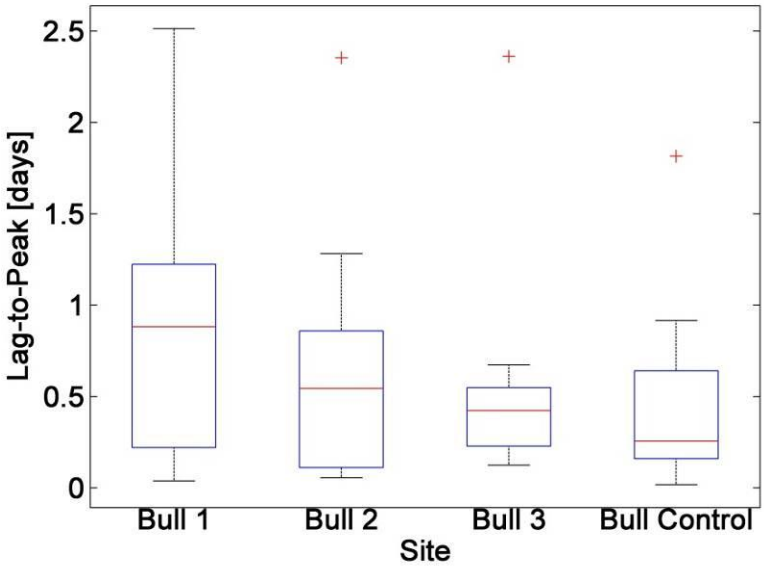

Figure 9: Box plot of lag-to-peak for selected storms

The lag-to-peak for Bull 1 has the largest variability (Figure 9) because it has the highest proportion of watershed area in high elevations. We assume that precipitation often occurs in the form of snow, which delays the lag-to-peak time. Bull 3 again has the lowest variability, due to its perennial nature. Bull Control has larger variability than Bull 3, but a lower median value, possibly due to its tipping bucket location at the outlet.

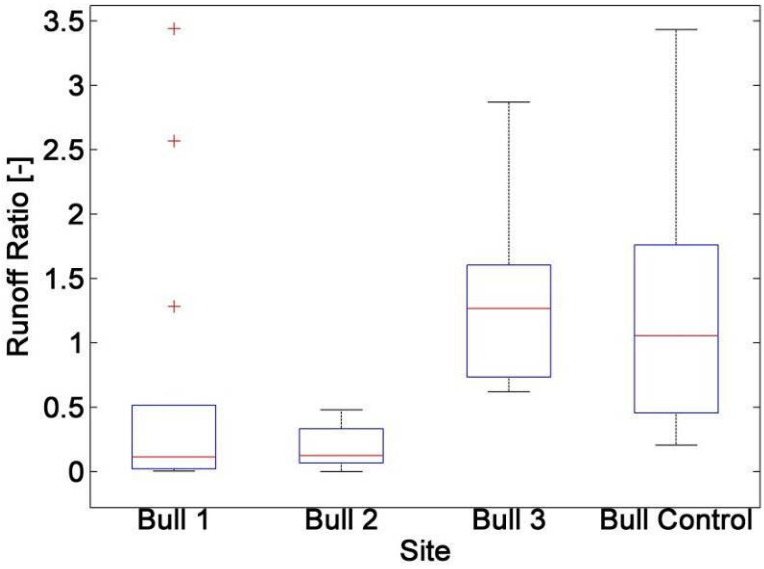

Figure 10: Box plot of runoff ratio for selected storms

There is high variability in the runoff ratios (Figure 10). Despite being unburned, Bull Control is did not have the lowest variability in runoff. This can be attributed to the location of the tipping bucket (watershed outlet) and snow storms in the upper portion of the watershed. Snow stored in the snowpack can melt during the winter and spring, which is an unaccounted input into the system. If a melt is in progress and a storm occurs, water input could exceed water outlet, which yields a theoretically impossible runoff ratio. To determine if snow is occurring at the time of a storm event, temperature recorded at the watershed's air HOBO was extrapolated to the watershed peak temperature via the adiabatic lapse rate of -9.8 °C/km. Precipitation is matched with the temperature timeseries and precipitation occurring at temperatures less than 0 °C is assumed snow (Appendix K). Bull 2 has the lowest variability in runoff ratios because its

tipping bucket is centrally located within the watershed. Bull 1 has three outliers likely because of snowfall during the storm.

A timeseries of the three storm parameters shows their variability over time (Figures 11-13). Following a wildfire, the response lag and lag-to-peak are expected to be low and increase as the watershed recovers. However, response lag initially starts high and then generally decreases over time, while the lag-to-peak has no apparent consistency. Values are at a minimum in the summer months, when the soil is dry and snowfall is not possible. These variables may be influenced by time between storms, rainfall intensity, and location. When the time between storms is small, the soil moisture is high and rainfall runs off rather than infiltrate the soil. For example, Storm 3 has a low lag-to-peak time because the time between Storm 2 was two days.

Runoff ratios should follow the opposite pattern, where runoff ratios are initially high and then decrease. Bull 3 and Bull Control frequently have runoff ratios greater than one, which can again be attributed to the location of the tipping bucket. Since the instrument was located at the outlet, the rainfall pattern is assumed to be constant across the entire watershed. The lack of data in the upper watershed attributes to the abnormally high runoff ratios. Bull 1's runoff ratios appear to be affected by this as well for storms occurring in the early Spring 2011. Bull 2 has the most consistent and reasonable runoff ratios because its tipping bucket was centrally located in the watershed.

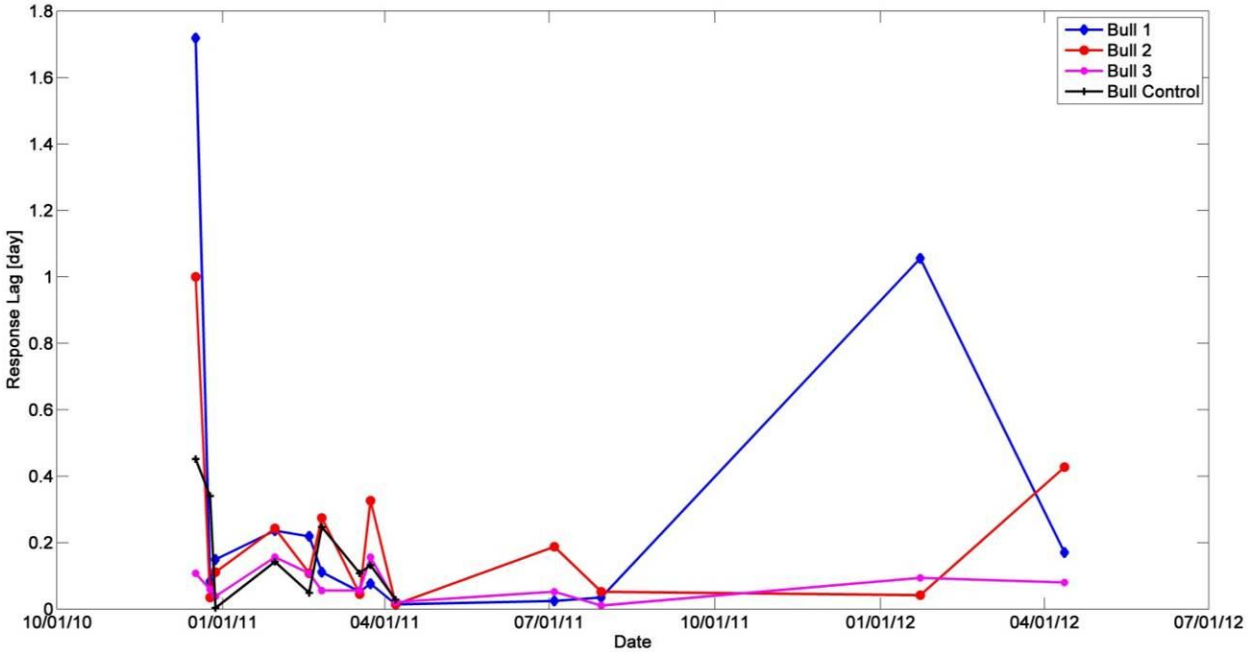

Figure 11: Response lag timeseries for selected storms

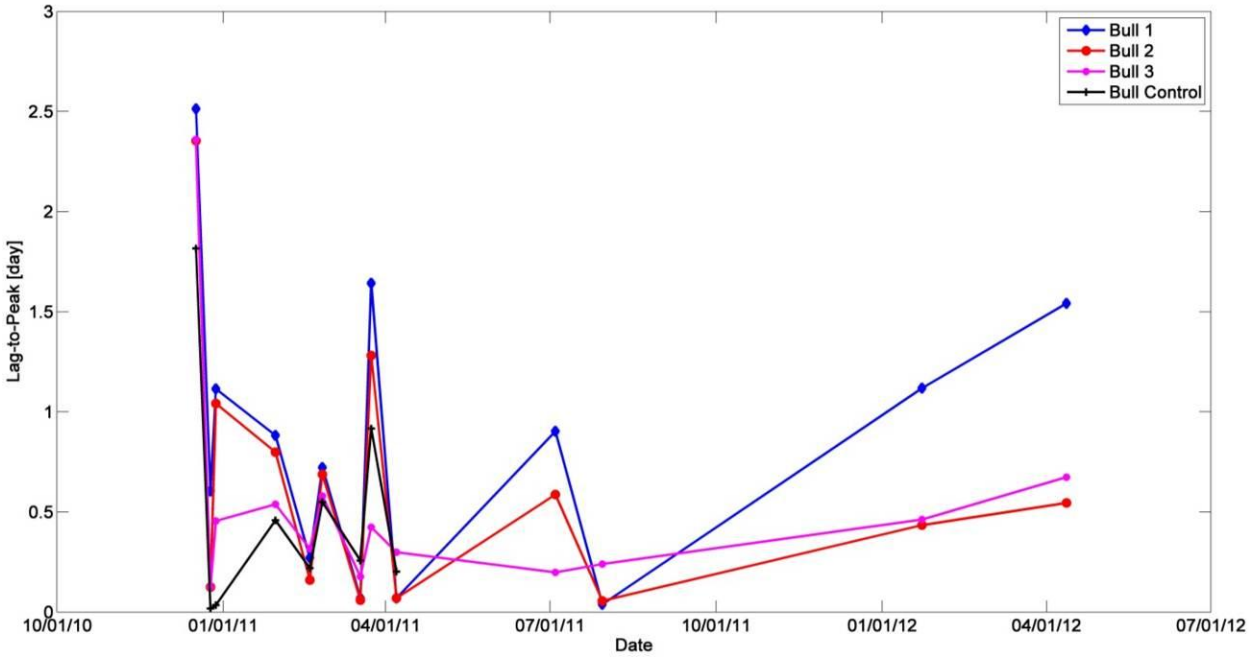

Figure 12: Lag-to-peak timeseries for selected storms

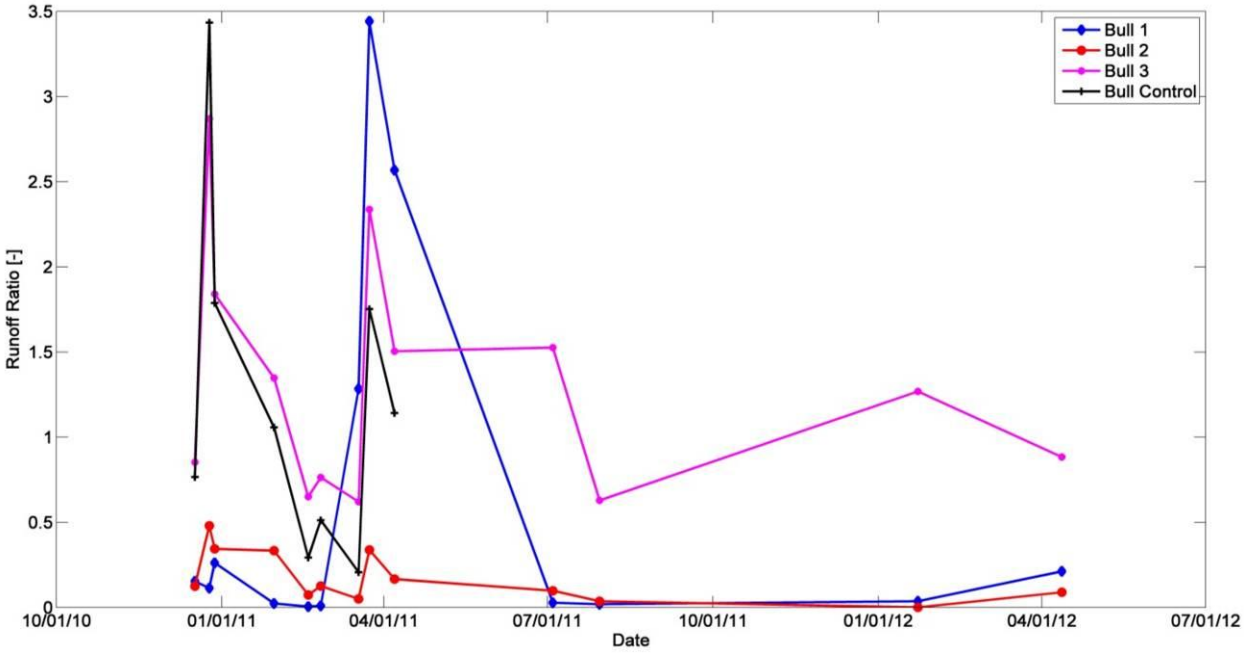

Figure 13: Runoff ratio timeseries for selected storms

Conclusions

Nearly two years of precipitation and five-minute discharge data was analyzed in this study. Precipitation data was consistent among sites at the daily level, and water year totals were similar to the Kern River Intake #3 gauge. Point precipitation measurements appear to miss localized storms common during the summer periods and skew our rainfall-runoff relationships. Similarly, snowfall that occurred in upper elevations of the sites was not measured and was roughly interpreted.

Cross-section changes occurred in a larger degree at wider cross-sections, such as Bull 1 and Bull 2. The largest cross-section change occurred early in the study period, likely due to top soil instability immediately following the wildfire. Bull 1, Bull 2, and Bull Control all experienced scouring, while Bull 3 was the only site to have sediment deposition early in the study period. Bull 3 has perennial flow with south and east dominant aspects, which is unique from the other study areas. Bull 3 also has the lowest watershed slope and a higher amount of boulders in the channel. These factors all combine to result in soil deposition at the cross-section.

Geomorphic parameters were analyzed in relation to area-normalized discharge. Aspect, soil type, and watershed shape have the largest impact on discharge. South aspects have higher runoff than other aspects, while north aspects have the smallest runoff. Type D soils also have higher runoff rates than Type C soils. Finally, narrow watersheds, such as Bull 3 and Bull Control, facilitate faster runoff and larger peak flows than more circular watersheds (Bull 1 and Bull 2). Slope was determined to not have a discernible effect on discharge. Pre-fire vegetation and burn severities were similar between the burned sites and no relationship was seen.

A selection of storms, predominantly from WY 2011, was analyzed to evaluate watershed recovery based on the rainfall-runoff response. Uncertainties in precipitation at the upper elevations of Bull 1, Bull 3, and Bull Control carried into the evaluation of the storm hydrographs. The response lag, lag-to-peak, and runoff ratio for each storm were analyzed for variability within and between sites, and a timeseries was plotted to track changes over time. Bull 3 had less variability in response time and lag-to-peak likely because of its perennial stream, but the watershed aspect and slope could also be a factor. Bull 2 has the least variability in the runoff ratio because the tipping bucket was located in the middle of the watershed and provided a more accurate estimate of the rainfall over the entire study site. When tracking the variable changes over time to judge watershed recovery, no conclusion could be drawn as the variables seem to be heavily dependent on the precipitation type and the time between storms. If snowfall occurred in the upper watershed elevations, data became severely skewed. Additionally, if the time between storms was short, then the corresponding response lag and lag-to-peak were much shorter.

Future direction of this work involves relating the hydrologic analysis presented in this report with remote sensing data from Landsat 7. The remote sensing top of atmosphere radiance will be converted to above ground reflectance and atmospherically corrected using the 6S model. Once the corrected reflectance is obtained, the Normalized Difference Vegetation Index (NDVI) will be calculated for all available images. The goal is to track vegetation recovery through NDVI and correlate it with storm rainfall-runoff response. Additionally, more storm parameters will be analyzed to evaluate watershed recovery.

Appendix

Appendix A – Pre-fire land cover

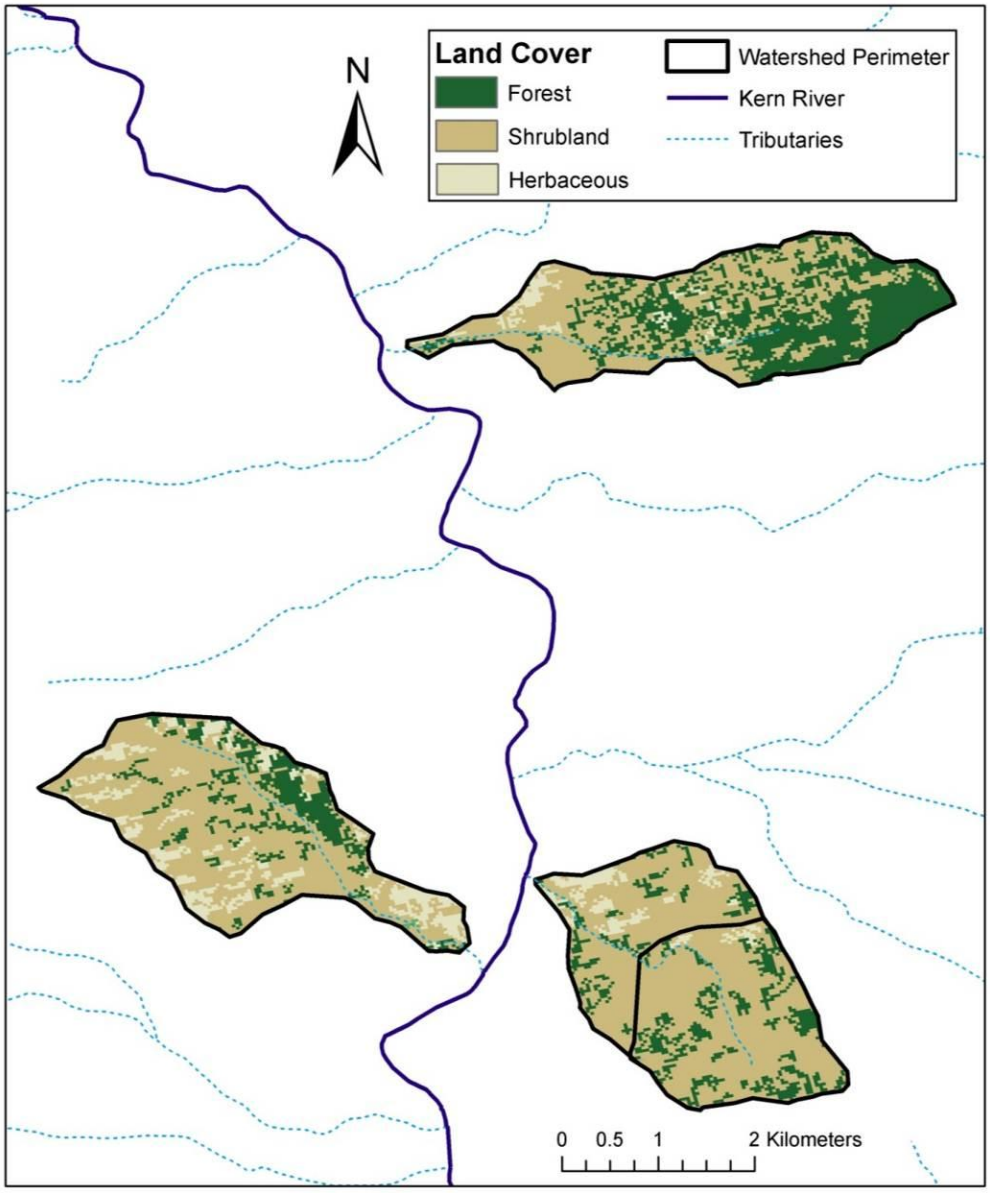

Appendix B – Instrument location and site aspect

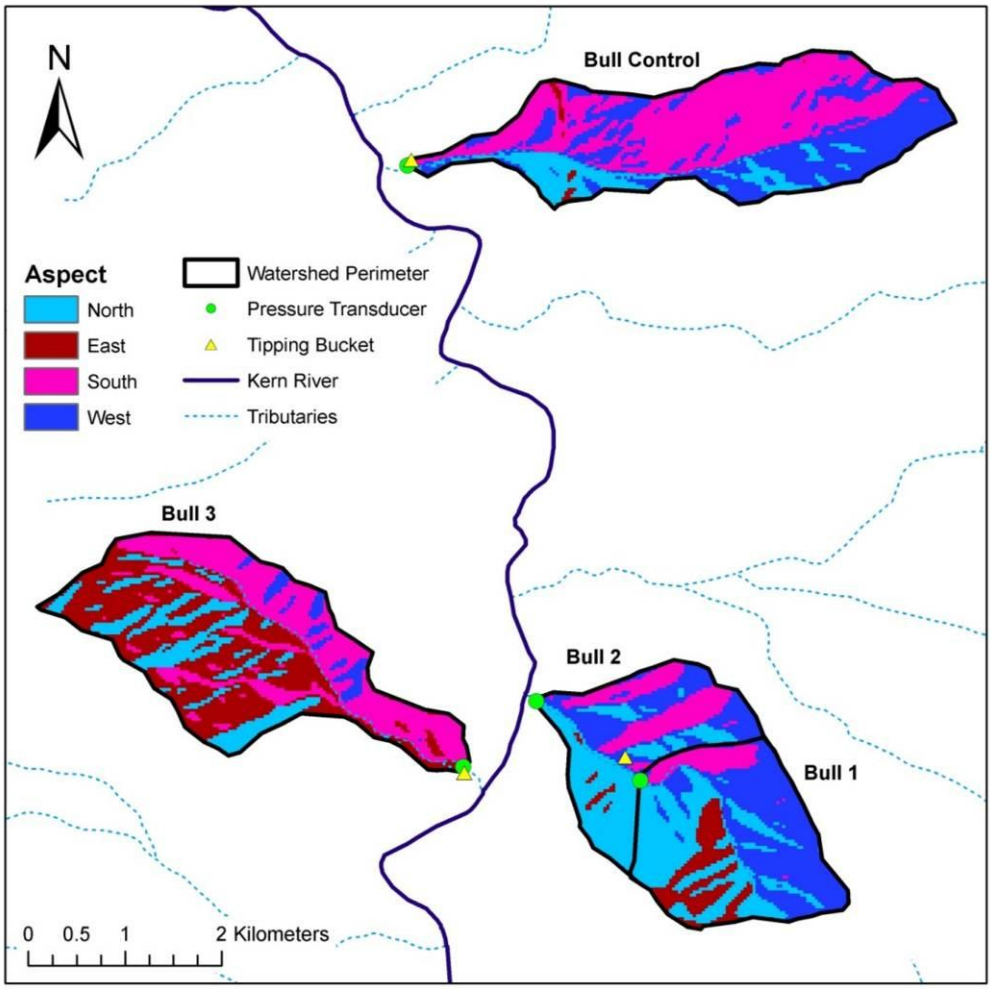

Appendix C – HOBO instrumentation method

To deploy the HOBO in the channel, the HOBO was housed in a 38.1mm PVC pipe with approximately ten 6.35 to 12.7mm holes drilled into the pipe (Figure 3). The pipe was capped at both ends and the HOBO was suspended with zip-ties through the holes. The HOBO house allowed for water to enter the housing while protecting the pressure transducer from debris. To install the HOBO and HOBO house in the channel, a fence post was hammered into the deepest point of the channel cross-section.

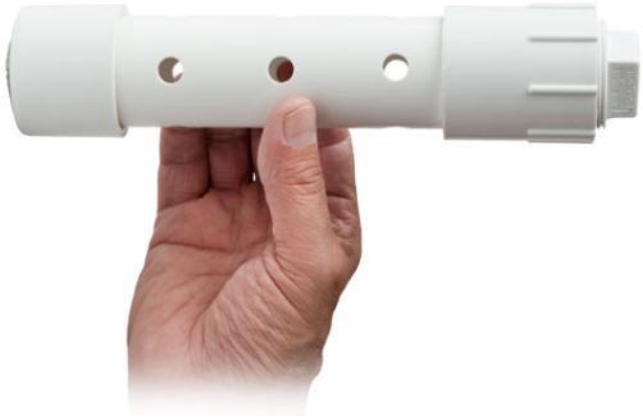

Example HOBO house (Onset, 2012)

Appendix D – Air pressure interpolation at Bull 1 and Bull Control from Bull 2

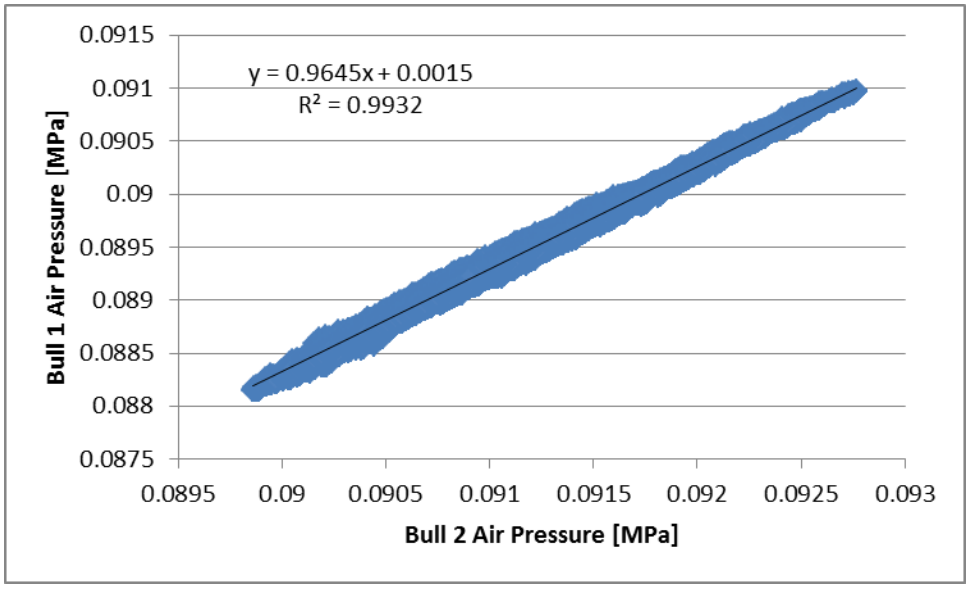

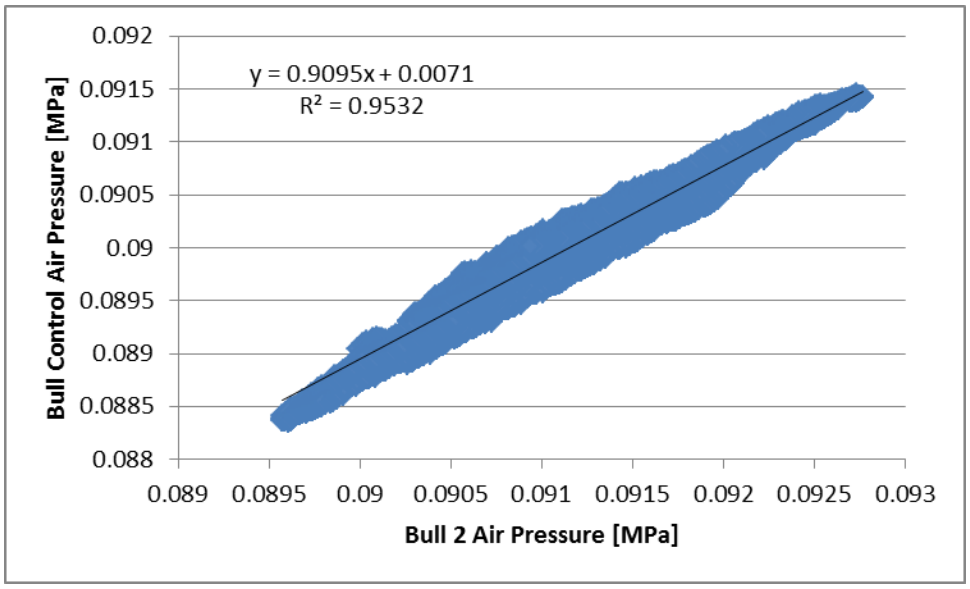

Appendix E – Rating curves

Bull 2:

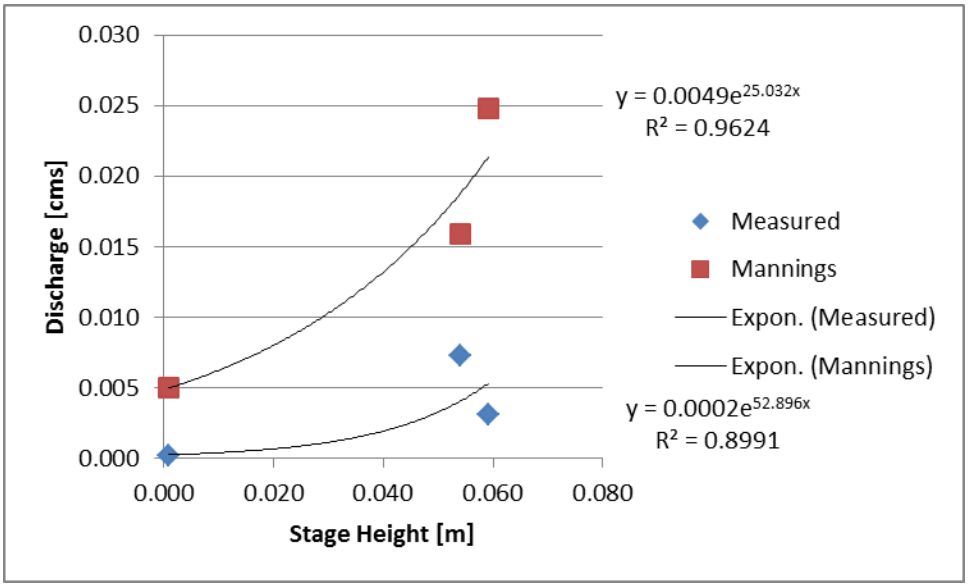

Bull 3:

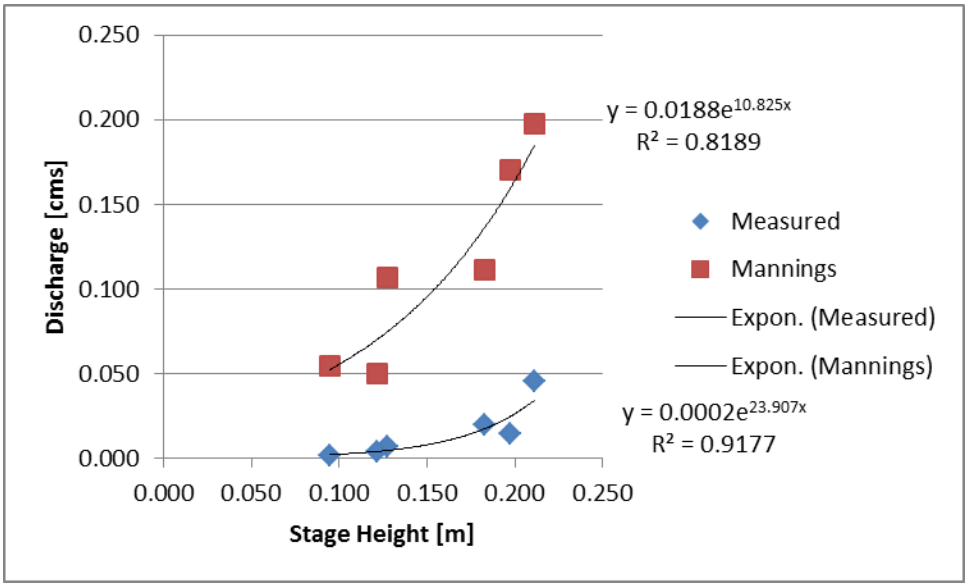

Bull Control:

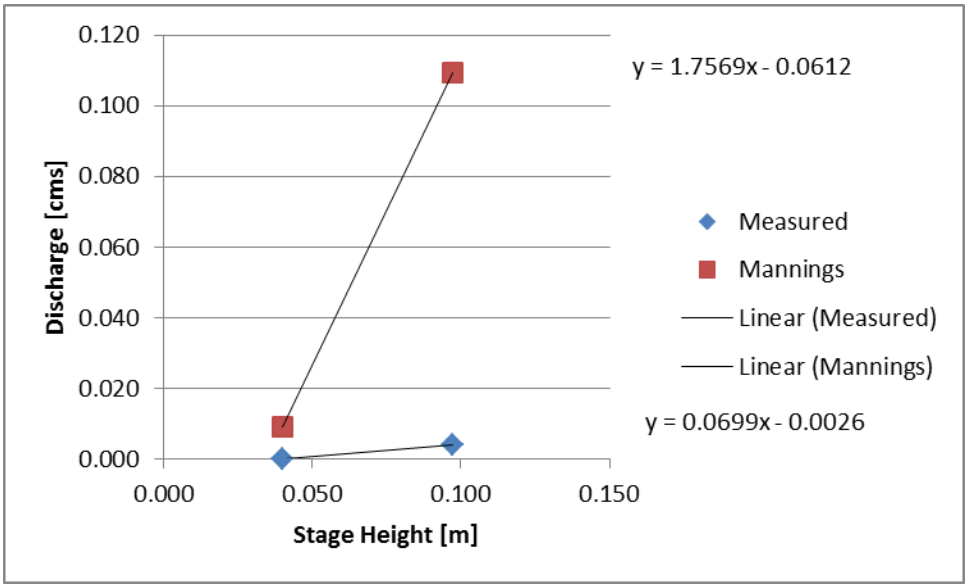

Appendix F – Precipitation timeseries for study sites

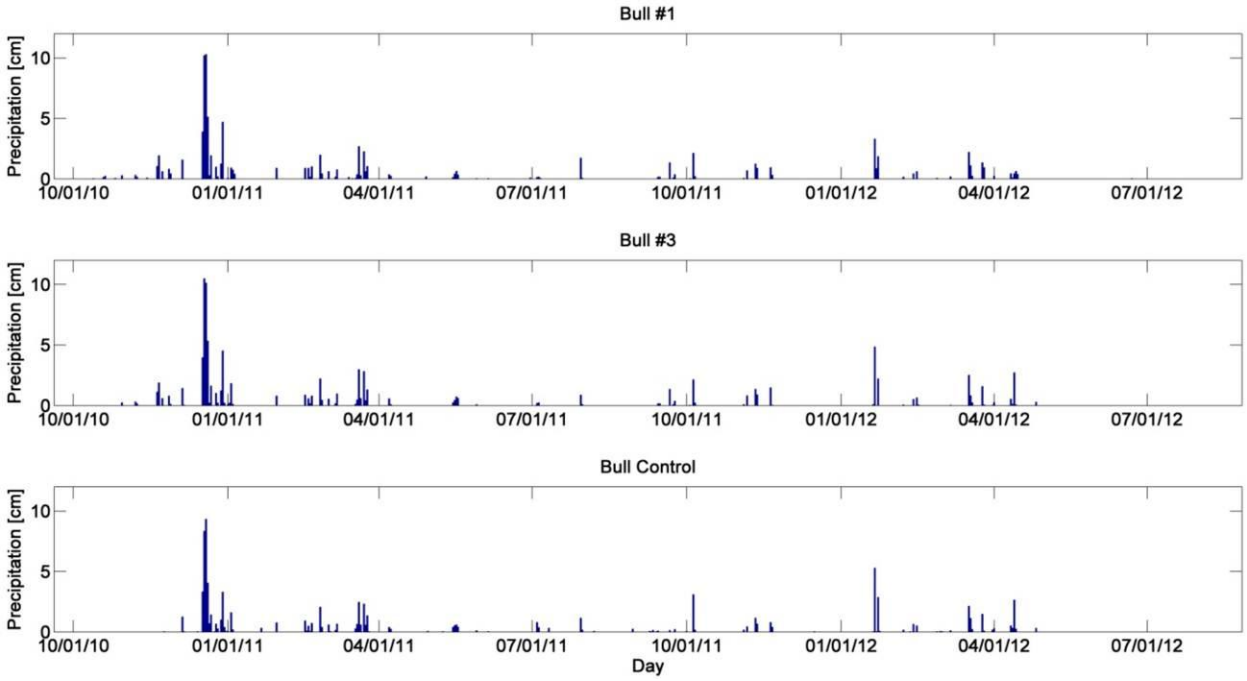

Appendix G – Measured cross-sections with each visit

Note: All figures are looking upstream, with the left-bank on the left. The dark black line represents current visit cross-section and light black line represents previous visit. For example: Visit 2 (top left of figures), the dark line is the Visit 2 cross-section measurement and the light line is the Visit 1 cross-section measurement.

Bull 1:

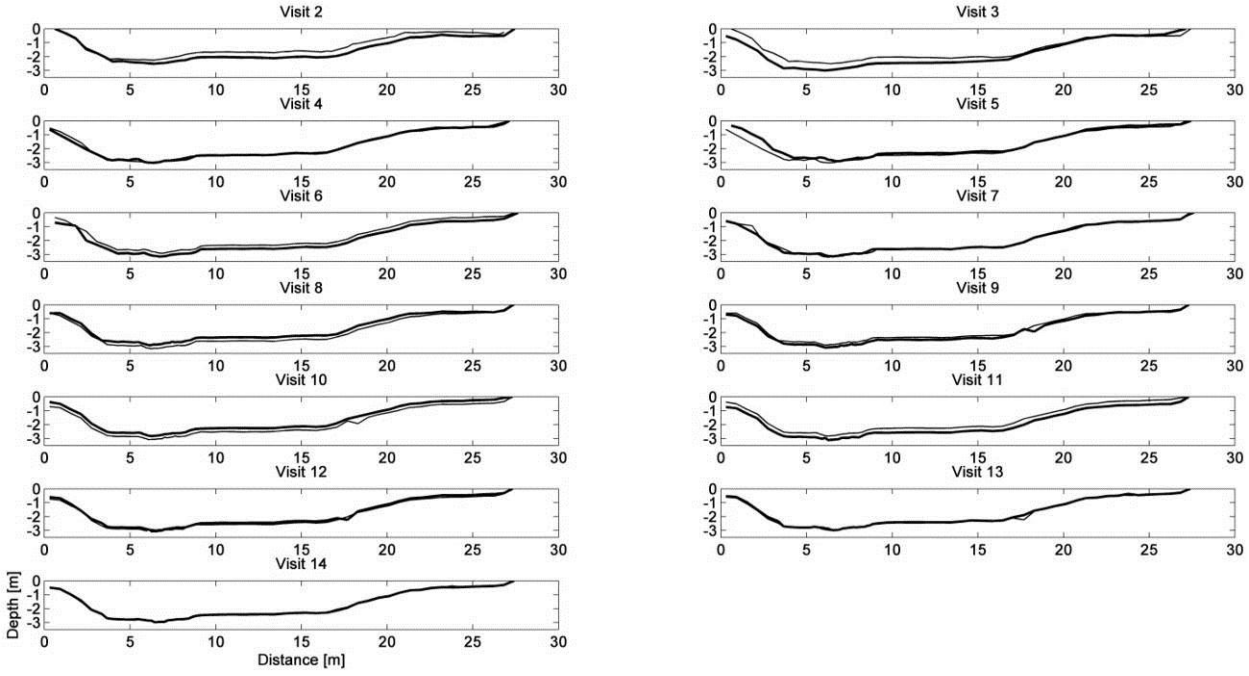

Bull 2:

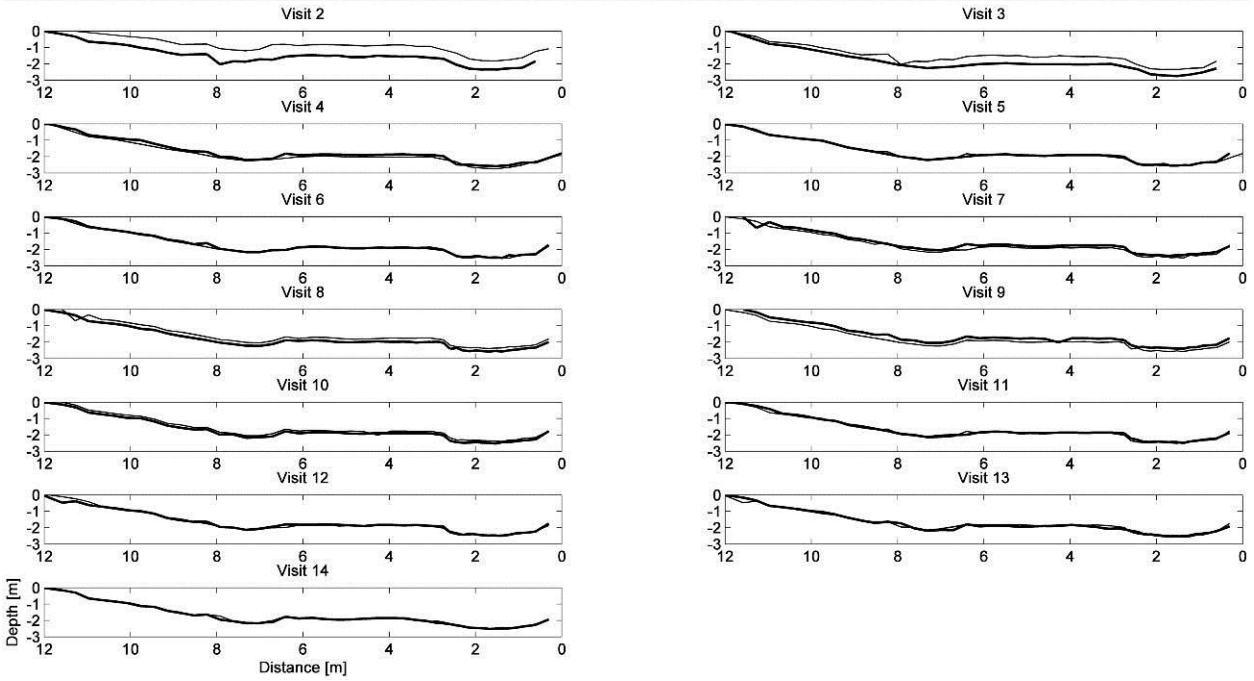
Visit 2
Visit 3
Visit 4
Visit 5
Visit 6
Visit 7
Visit 8
Visit 9
Visit 10
Visit 11
Visit 12
Visit 13
Visit 14
Depth [m]
Distance [m]

Bull 3:

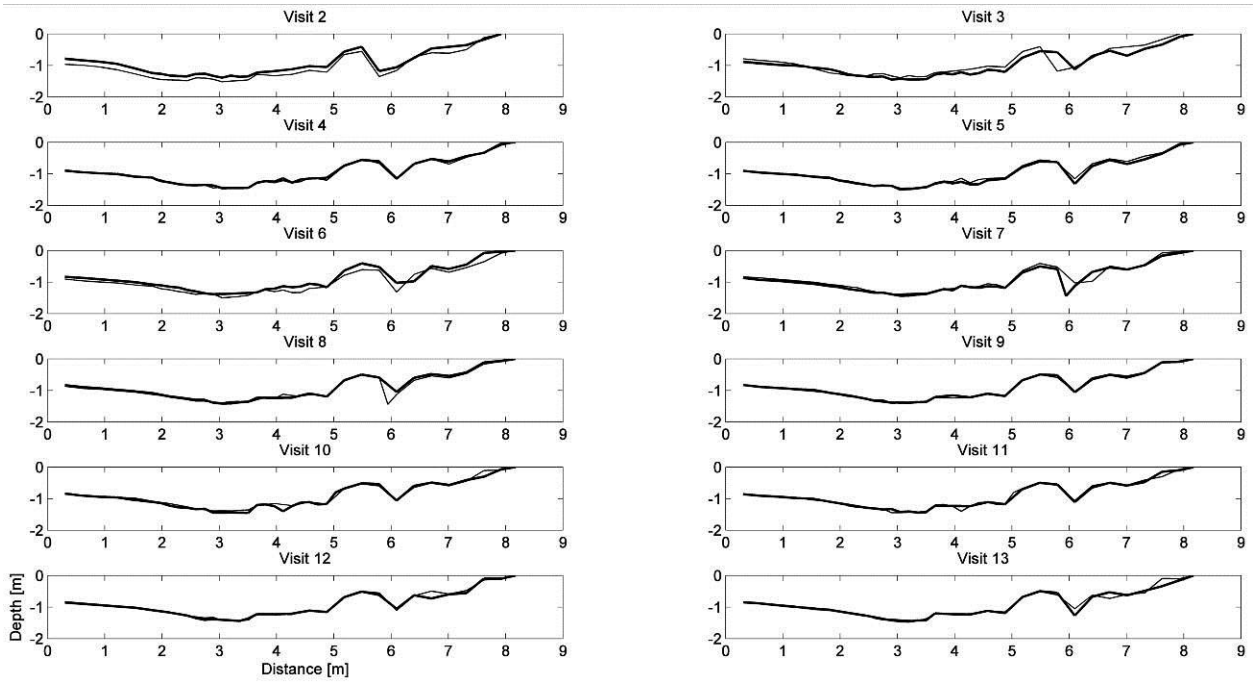
Visit 2
Visit 3
Visit 4
Visit 5
Visit 6
Visit 7
Visit 8
Visit 9
Visit 10
Visit 11
Visit 12
Visit 13
Depth [m]
Distance [m]

Bull Control:

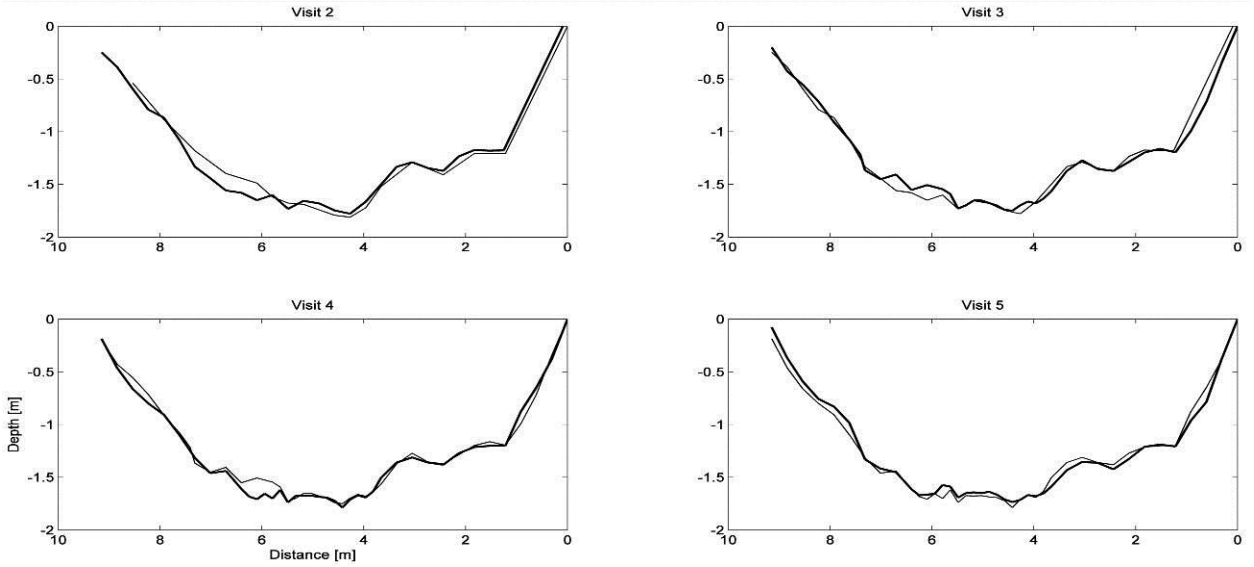

Appendix H – Precipitation and cross-section area change

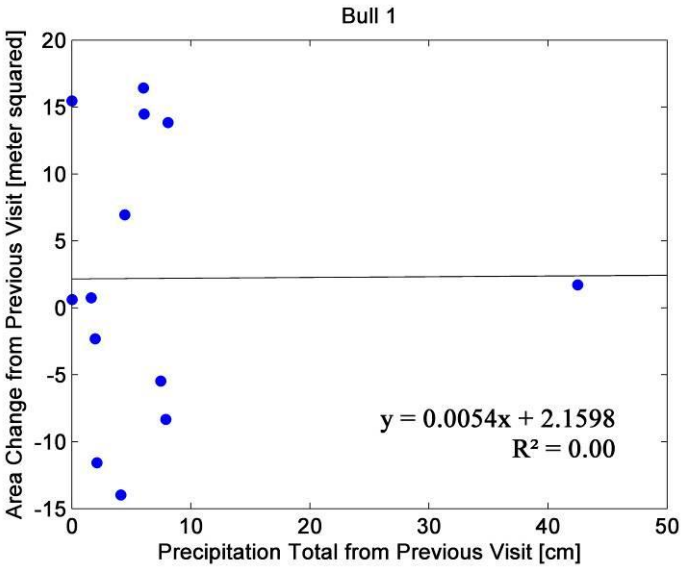

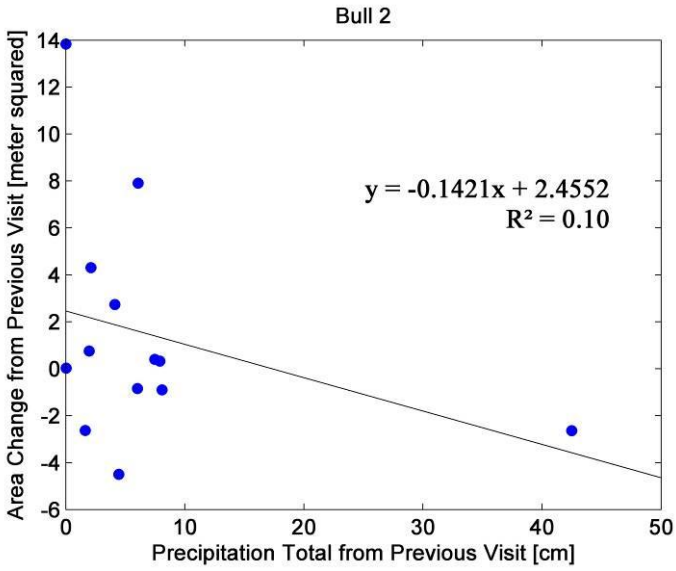

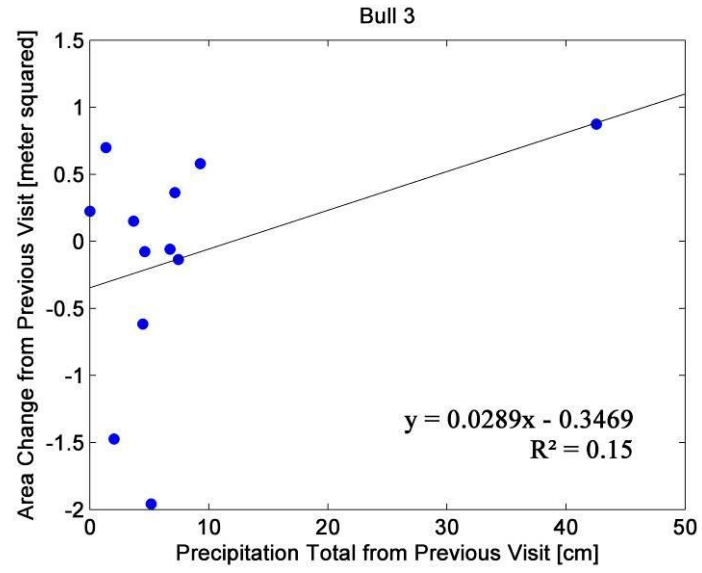
Bull 3
Area Change from Previous Visit [meter squared]
Precipitation Total from Previous Visit [cm]
y = 0.0289x - 0.3469
R² = 0.15

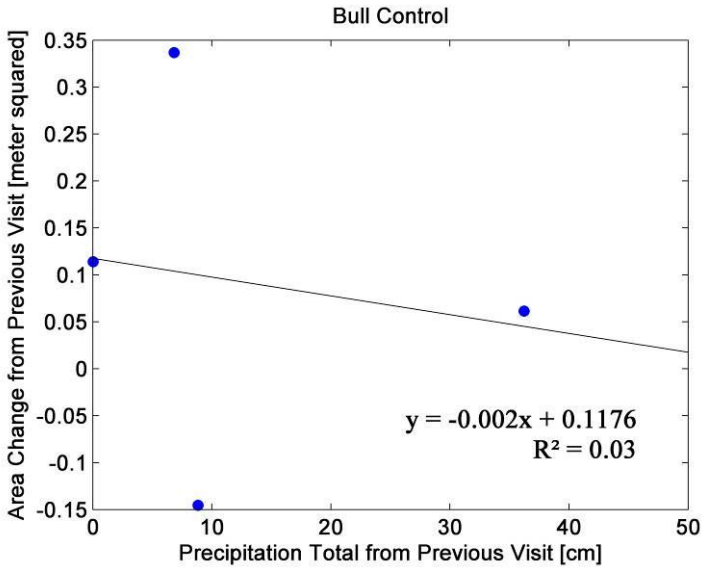
Bull Control
Area Change from Previous Visit [meter squared]
Precipitation Total from Previous Visit [cm]
y = -0.002x + 0.1176
R² = 0.03

Appendix I – Discharge and precipiation time series

Bull 1:

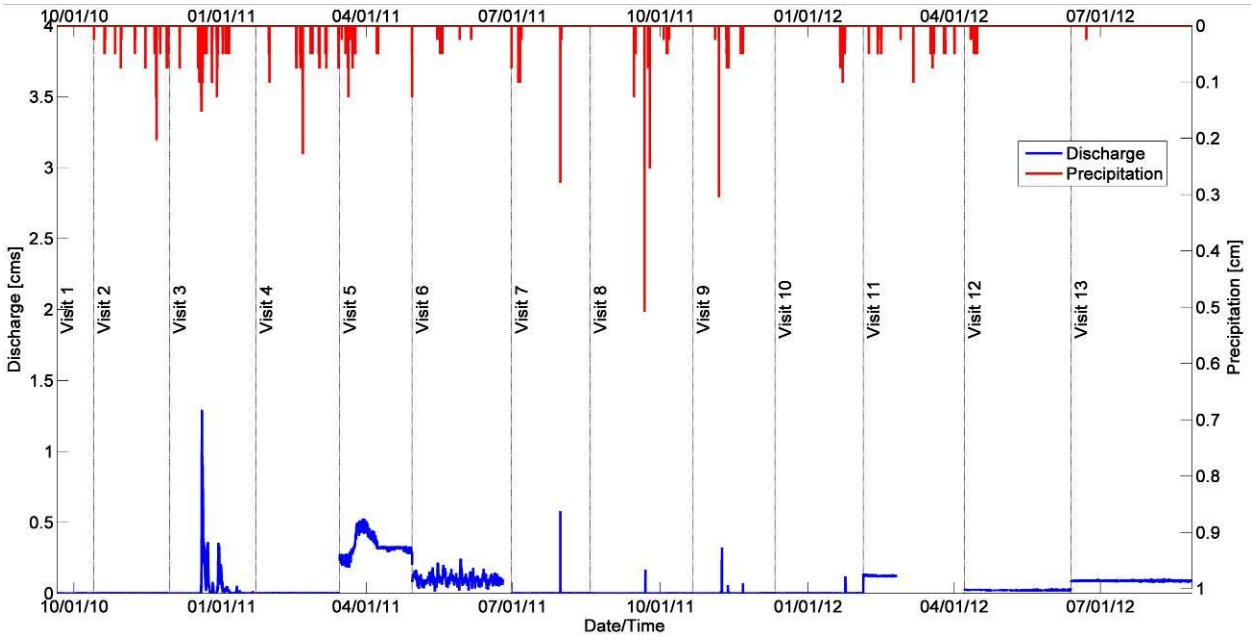

Bull 2:

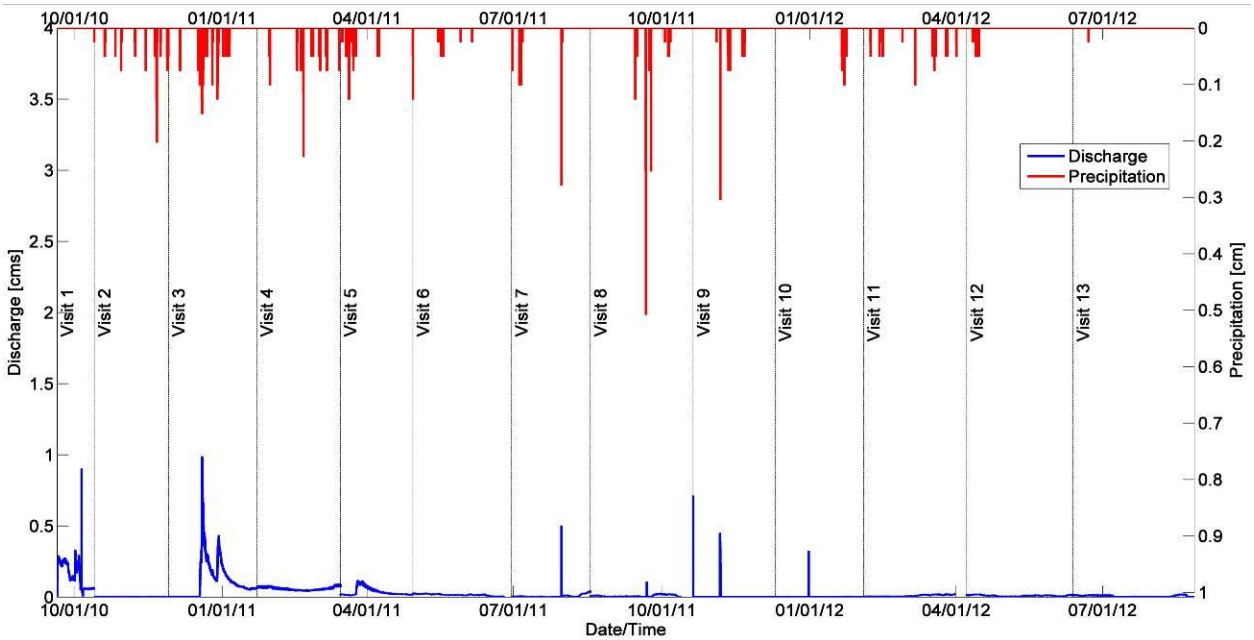

Bull 3:

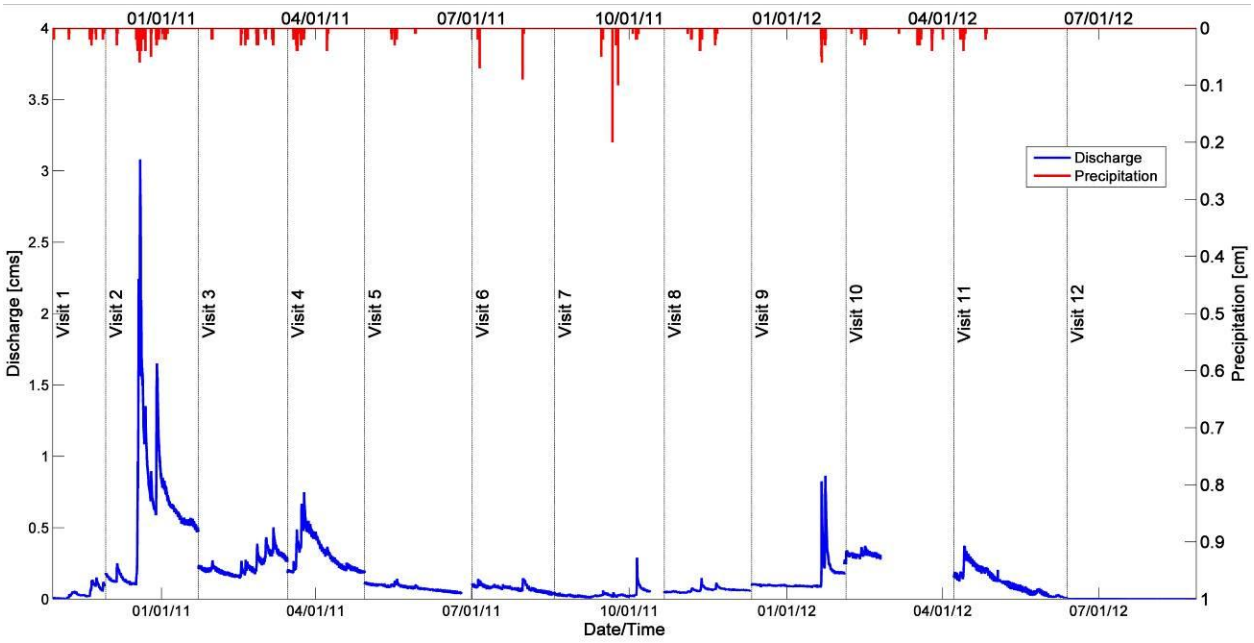

Bull Control:

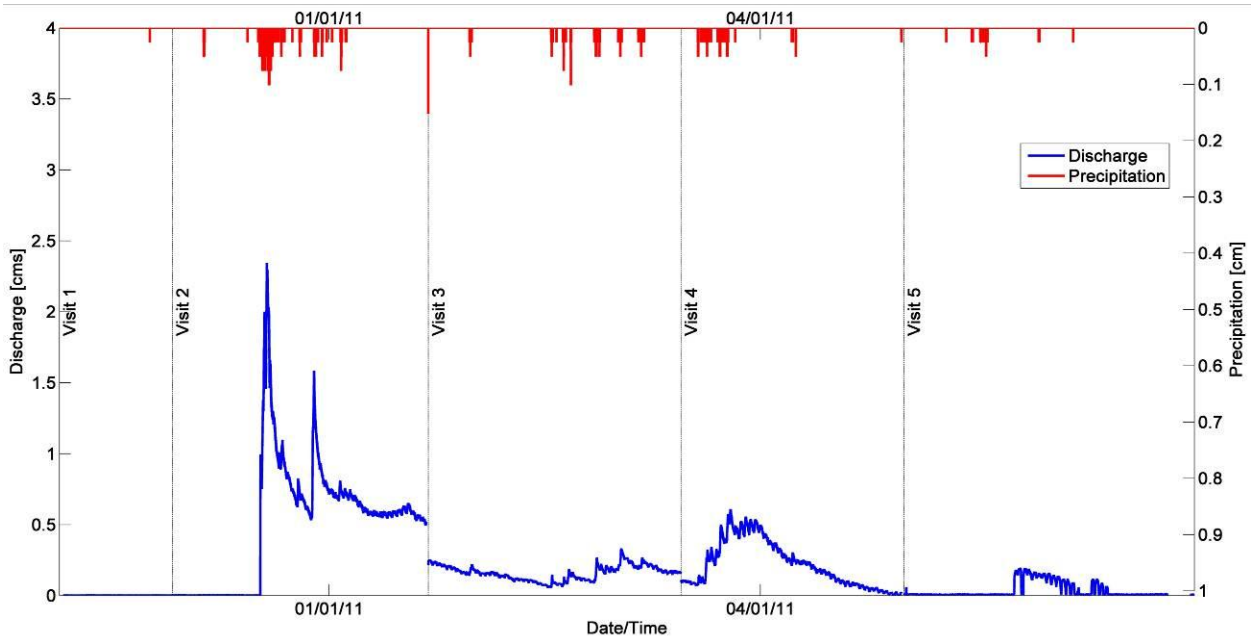

Appendix J – Storm data

Legend: t_{w0} = beginning of effective water input (days), t_{we} = end of effective water input (days), t_{pk} = time of peak discharge (days), T_W = duration of effective water input (days), T_{LR} = response lag (days), T_{LP} = response lag (days), I = intensity (cm/day), RO = runoff ratio (-)

Storm 1:

	Bull 1	Bull 2	Bull 3	Bull Control
t_{w0}	12/17/2010 04:50	12/17/2010 04:50	12/17/2010 04:40	12/17/2010 04:35
t_{we}	12/21/2010 01:15	12/21/2010 01:15	12/21/2010 01:45	12/21/2010 10:10
t_{pk}	12/19/2010 17:10	12/19/2010 13:20	12/19/2010 13:20	12/19/2010 00:10
T_w	3.85	3.85	3.88	4.23
T_{LR}	1.72	1.00	0.11	0.45
T_{LP}	2.51	2.35	2.36	1.82
I	7.69	7.69	7.73	6.04
RO	0.15	0.13	0.85	0.77

Storm 2:

	Bull 1	Bull 2	Bull 3	Bull Control
t_{w0}	12/25/2010 19:20	12/25/2010 19:20	12/25/2010 20:10	12/25/2010 19:30
t_{we}	12/26/2010 03:40	12/26/2010 03:40	12/26/2010 03:45	12/26/2010 02:55
t_{pk}	12/26/2010 09:50	12/25/2010 22:20	12/25/2010 23:10	12/25/2010 19:55
T_w	0.35	0.35	0.32	0.31
T_{LR}	0.08	0.03	0.06	0.34
T_{LP}	0.60	0.12	0.12	0.02
I	3.36	3.36	3.86	2.96
RO	0.11	0.48	2.87	3.43

Storm 3:

	Bull 1	Bull 2	Bull 3	Bull Control
t_{w0}	12/28/2010 20:20	12/28/2010 20:20	12/28/2010 20:15	12/28/2010 20:10
t_{we}	12/29/2010 17:25	12/29/2010 17:25	12/29/2010 19:00	12/29/2010 16:50
t_{pk}	12/29/2010 23:05	12/29/2010 21:20	12/29/2010 07:10	12/28/2010 21:00
T_w	0.88	0.88	0.95	0.86
T_{LR}	0.15	0.11	0.04	0.00
T_{LP}	1.11	1.04	0.45	0.03
I	6.77	6.77	6.06	4.98
RO	0.26	0.34	1.84	1.79

Storm 4:

	Bull 1	Bull 2	Bull 3	Bull Control
t_{w0}	01/30/2011 07:30	01/30/2011 07:30	01/30/2011 07:25	01/30/2011 07:15
t_{we}	01/30/2011 18:00	01/30/2011 18:00	01/30/2011 17:50	01/30/2011 18:00
t_{pk}	01/31/2011 04:40	01/31/2011 02:40	01/30/2011 20:20	01/30/2011 18:15
T_w	0.44	0.44	0.43	0.45
T_{LR}	0.24	0.24	0.16	0.14
T_{LP}	0.88	0.80	0.54	0.46
I	2.03	2.03	1.81	1.70
RO	0.02	0.33	1.35	1.06

Storm 5:

	Bull 1	Bull 2	Bull 3	Bull Control
t_{w0}	02/18/2011 19:00	02/18/2011 19:00	02/18/2011 19:00	02/18/2011 19:10
t_{we}	02/18/2011 23:30	02/18/2011 23:30	02/18/2011 23:25	02/18/2011 23:35
t_{pk}	02/19/2011 01:30	02/18/2011 22:50	02/19/2011 02:35	02/19/2011 00:25
T_w	0.19	0.19	0.18	0.18
T_{LR}	0.22	0.11	0.11	0.05
T_{LP}	0.27	0.16	0.32	0.22
I	4.74	4.74	3.04	2.62
RO	0.01	0.07	0.65	0.29

Storm 6:

	Bull 1	Bull 2	Bull 3	Bull Control
t_{w0}	02/25/2011 07:45	02/25/2011 07:45	02/25/2011 07:40	02/25/2011 07:50
t_{we}	02/25/2011 22:00	02/25/2011 22:00	02/25/2011 23:00	02/26/2011 01:25
t_{pk}	02/26/2011 01:05	02/26/2011 00:15	02/25/2011 21:35	02/25/2011 21:00
T_w	0.59	0.59	0.64	0.73
T_{LR}	0.11	0.27	0.06	0.25
T_{LP}	0.72	0.69	0.58	0.55
I	3.34	3.34	3.46	2.84
RO	0.01	0.13	0.76	0.51

Storm 7:

	Bull 1	Bull 2	Bull 3	Bull Control
t_{w0}	03/18/2011 23:45	03/18/2011 23:45	03/18/2011 23:30	03/18/2011 22:35
t_{we}	03/19/2011 01:35	03/19/2011 01:35	03/19/2011 01:15	03/19/2011 02:00
t_{pk}	03/19/2011 01:25	03/19/2011 01:10	03/19/2011 03:45	03/19/2011 04:45
T_w	0.08	0.08	0.07	0.14
T_{LR}	0.05	0.05	0.06	0.11
T_{LP}	0.07	0.06	0.18	0.26
I	4.32	4.32	6.27	4.64
RO	1.28	0.05	0.62	0.21

Storm 8:

	Bull 1	Bull 2	Bull 3	Bull Control
t_{w0}	03/24/2011 21:45	03/24/2011 21:45	03/24/2011 19:35	03/24/2011 19:40
t_{we}	03/25/2011 06:15	03/25/2011 06:15	03/25/2011 06:40	03/25/2011 06:45
t_{pk}	03/26/2011 13:10	03/26/2011 04:30	03/25/2011 05:45	03/25/2011 17:40
T_w	0.35	0.35	0.46	0.46
T_{LR}	0.08	0.33	0.16	0.13
T_{LP}	1.64	1.28	0.42	0.92
I	3.73	3.73	3.47	3.91
RO	3.44	0.34	2.34	1.75

Storm 9:

	Bull 1	Bull 2	Bull 3	Bull Control
t_{w0}	04/07/2011 13:10	04/07/2011 13:10	04/07/2011 13:05	04/07/2011 12:55
t_{we}	04/07/2011 16:25	04/07/2011 16:25	04/07/2011 18:50	04/07/2011 18:10
t_{pk}	04/07/2011 14:50	04/07/2011 14:50	04/07/2011 20:15	04/07/2011 17:45
T_w	0.14	0.14	0.24	0.22
T_{LR}	0.01	0.01	0.02	0.03
T_{LP}	0.07	0.07	0.30	0.20
I	2.63	2.63	2.33	1.74
RO	2.57	0.17	1.50	1.14

Storm 10:

	Bull 1	Bull 2	Bull 3
t_{w0}	07/04/2011 15:25	07/04/2011 15:25	07/04/2011 14:50
t_{we}	07/04/2011 15:30	07/04/2011 15:30	07/04/2011 15:35
t_{pk}	07/05/2011 13:05	07/05/2011 05:30	07/04/2011 19:35
T_w	0.00	0.00	0.03
T_{LR}	0.02	0.19	0.05
T_{LP}	0.90	0.59	0.20
I	36.58	36.58	5.69
RO	0.03	0.10	1.53

Storm 11:

	Bull 1	Bull 2	Bull 3
t_{w0}	07/30/2011 17:45	07/30/2011 17:45	07/30/2011 17:45
t_{we}	07/30/2011 19:40	07/30/2011 19:40	07/30/2011 19:25
t_{pk}	07/30/2011 18:40	07/30/2011 19:05	07/30/2011 23:30
T_w	0.08	0.08	0.07
T_{LR}	0.03	0.05	0.01
T_{LP}	0.04	0.06	0.24
I	21.63	21.63	12.44
RO	0.02	0.04	0.63

Storm 12:

	Bull 1	Bull 2	Bull 3
t_{w0}	01/23/2012 02:10	01/23/2012 02:10	01/23/2012 01:55
t_{we}	01/23/2012 23:55	01/23/2012 23:55	01/23/2012 17:55
t_{pk}	01/24/2012 05:00	01/23/2012 12:35	01/23/2012 13:00
T_w	0.91	0.91	0.67
T_{LR}	1.06	0.04	0.09
T_{LP}	1.12	0.43	0.46
I	2.05	2.05	3.31
RO	0.04	0.00	1.27

Storm 13:

	Bull 1	Bull 2	Bull 3
t_{w0}	04/12/2012 22:55	04/12/2012 22:55	04/12/2012 22:30
t_{we}	04/15/2012 06:20	04/15/2012 06:20	04/13/2012 18:00
t_{pk}	04/14/2012 11:55	04/13/2012 12:00	04/13/2012 14:40
T_w	2.31	2.31	0.81
T_{LR}	0.17	0.43	0.08
T_{LP}	1.54	0.55	0.67
I	0.65	0.65	3.53
RO	0.21	0.09	0.88

Appendix K – Precipitation and temperature at watershed peak timeseries

Bull 1:

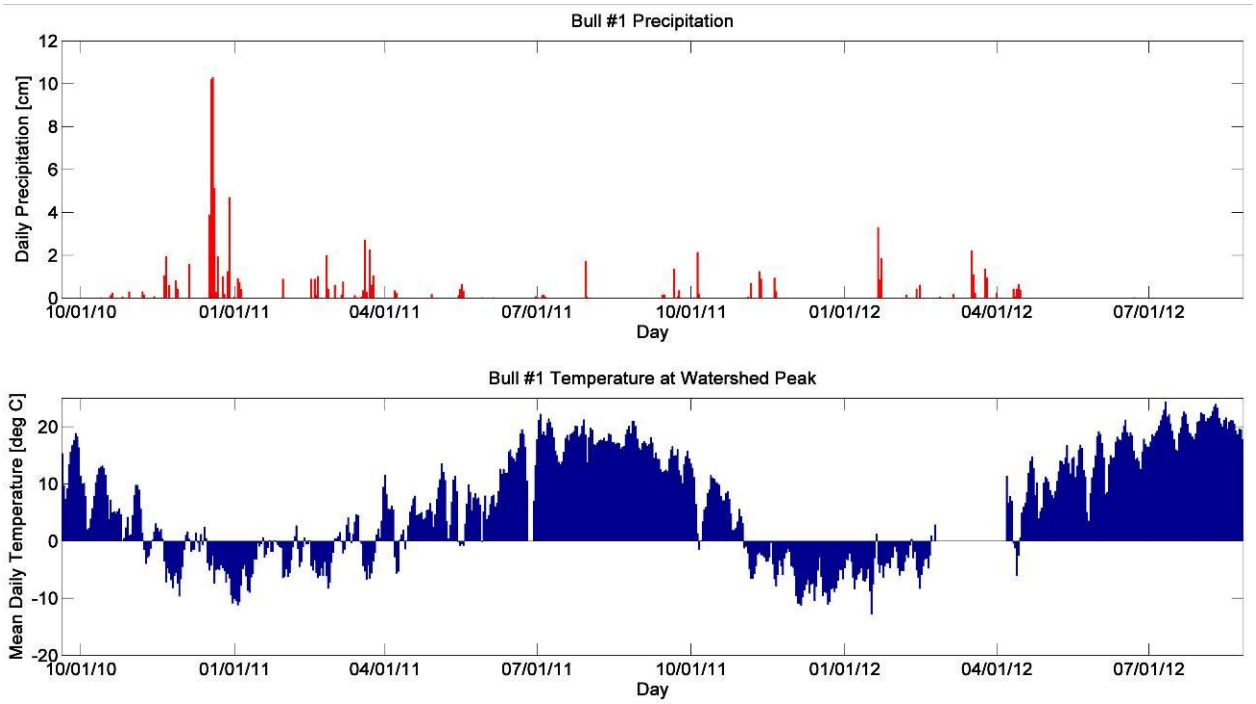

Bull 3:

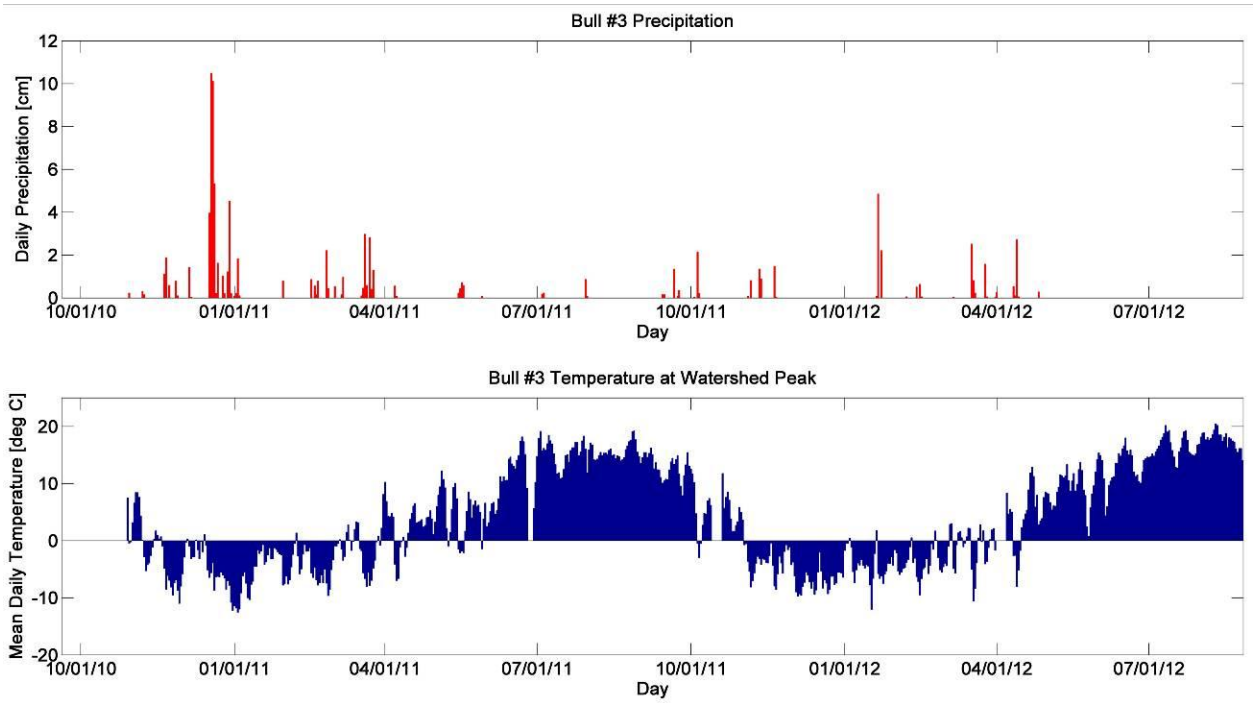
Bull #3 Precipitation
Daily Precipitation [cm]
12
10
8
6
4
2
0
10/01/10
01/01/11
04/01/11
07/01/11
10/01/11
01/01/12
04/01/12
07/01/12
Day
Bull #3 Temperature at Watershed Peak
Mean Daily Temperature [deg C]
20
10
0
-10
-20
10/01/10
01/01/11
04/01/11
07/01/11
10/01/11
01/01/12
04/01/12
07/01/12
Day

Bull Control:

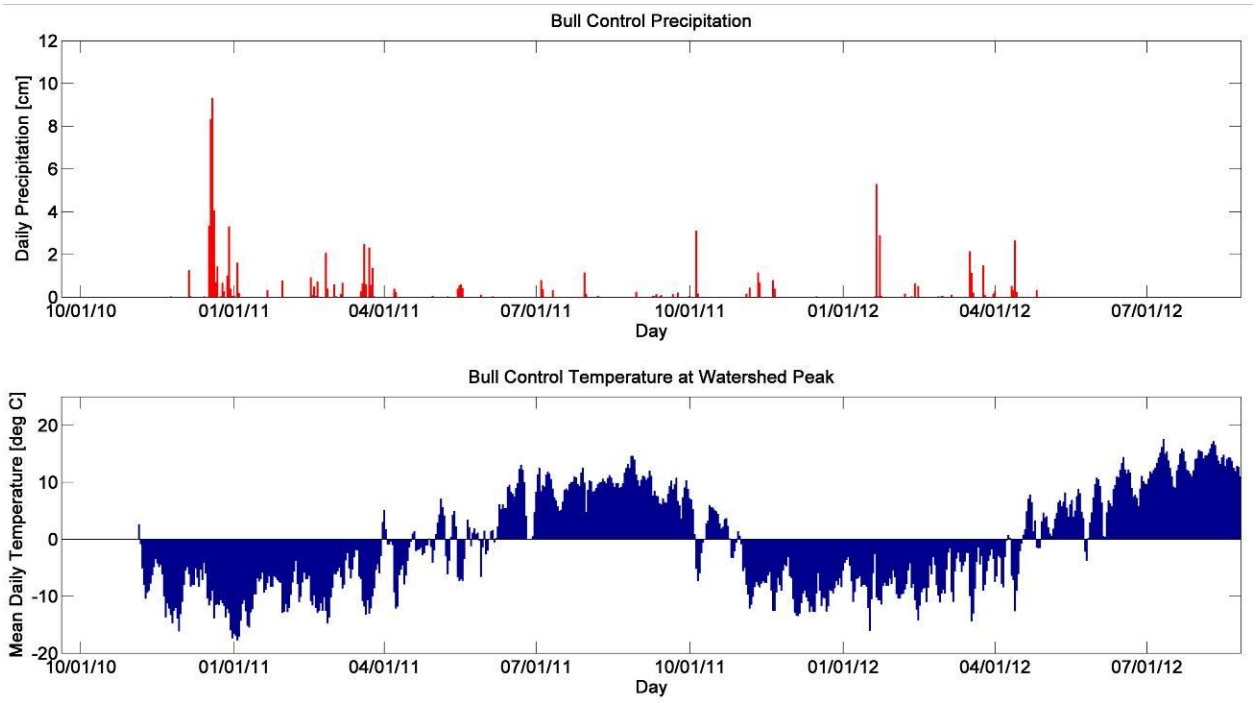

References

Baker, W.L. "Spatially heterogeneous multi-scale response of landscapes to fire suppression." *Oikos* 66 (1993): 66-71. Print.

Box, G.E.P., D.R. Cox. "An analysis of transformations." *Journal of the Royal Statistical Society Series B* 26.2 (1964): 211-252. Print.

Burke, M.P., T.S. Hogue, M. Ferreira, C.B. Mendez, B. Navarro, S. Lopez, J.A. Jay. "The Effect of Wildfire on Soil Mercury Concentrations in Southern California Watersheds." *Water, Air, & Soil Pollution* 212 (2010): 369-385. Print.

CA DWR CDEC. "Precipitation Averages." *Kern R Intake No. 3 (KR3)* (2012). Online. 29 Oct. 2012.

Casady, G.M., W.J.D. Leeuwen, S.E. Marsh. "Evaluating post-wildfire vegetation regeneration as a response to multiple environmental determinants." *Environmental Model Assessment* (2009). Doi: 10.1007/s10666-009-9210-x.

Chong, J., J. Renaud, E. Ailsworth. "Flash floods wash away lives, dreams." *Los Angeles Times* 03 Jan. 2004: All. Print.

Cydzik, K., T.S. Hogue. "Modeling postfire response and recovery using the hydrologic engineering center hydrologic modeling system (HEC-HMS)." *Journal of the American Water Resources Association* 45 (2009): 702-714. Print.

DeBano, L.F. "The role of file and soil heating on water repellency in wildland environments: a review." *Journal of Hydrology* 231-232 (2000): 195-206. Print.

Ebel, B.A., J.A. Moody, D.A. Martin. "Hydrologic conditions controlling runoff generation immediately after wildfire." *Water Resources Research* 48 (2012): 1-13. Online.

Fox, D.M., F. Darboux, P. Carrega. "Effects of fire-induced water repellency on soil aggregate stability, splash erosion and saturated hydraulic conductivity for different size fractions." *Hydrological Processes* 21 (2007): 2377-2384. Print.

FRAP. *Fire Perimeters.* California Department of Forestry and Fire Protection. 29 Mar. 2012. Web. 20 Sep. 2012.

Fry, J., G. Xian, S. Jin, J. Dewitz, C. Homer, L. Yang, C. Barnes, N. Herold, J. Wickham. "Completion of the 2006 National Land Cover Database for the Conterminous United States." *PE&RS* 77 (2011): 858-864. Print.

Gabet, E.J. "Post-fire thin debris flows: sediment transport and numerical modeling." *Earth Surface Processes and Landforms* 28 (2003): 1341-1348. Print.

Gesch, D.B., M. Oimoen, S. Greenlee, C. Nelson, M. Steuck, D. Tyler. "The National Elevation Dataset." *Photogrammatic engineering and remote sensing* 68 (2002): 1-5. Online.

Gilley, J.E., D.C. Flanagan, E.R. Kottwitz, M.A. Weltz. "Darcy-Weisbach roughness coefficients for overland flow." *Overland Flow: Hydraulic and Erosion Mechanics.* Parsons AJ Abrahams AD (eds.) Chapman & Hall: New York, NY (1992): 25-52. Print.

Hogue, T.S., S. Sorooshian, H. Gupta, A. Holz, D. Braatz. "A multistep automatic calibration scheme for river forecasting models." *Journal of Hydrometerology* 1.6 (2000): 524-542. Print.

Ice, G.G., D.G. Neary, P.W. Adams. "Effects of Wildfire on Soils and Watershed Processes." *Journal of Forestry* 102 (2004): 16-20. Print.

Jung, H.Y., T.S. Hogue, L.K. Rademacher, T. Meixner. "Impact of wildfire on source water contributions in Devil Creek, CA: evidence from end-member mixing analysis." *Hydrological Processes* 13 (2009): 183-200. Print.

Kauffman, J.B. "Death rides the forest – perceptions of fire, land use and ecological restoration of western forests." *Conversation Biology* 18 (2004): 878-882. Print.

Keeley, J.E., C.J. Fotheringham, M. Morais. "Reexamining fire suppression impacts on brushland fire regimes." *Science* 284 (1999): 1829-1832. Print.

Kinoshita, A.M., T.S. Hogue. "Spatial and temporal controls on post-fire hydrologic recovery in Southern California watersheds." *Catena* 87 (2011): 240-252. Print.

Kitzberger, T., P.M. Brown, E.K. Heyerdahl, T.W. Swetnam, T.T. Veblen. "Contingent Pacific-Atlantic Ocean influence on multi-century wildfire synchrony over western North America." *Proceedings of the National Academy of Sciences of the United States of America* 104.2 (2007): 543-548. Print.

Krammes, J.S., L.F. DeBano. "Soil Wettability: a neglected factor in watershed management." *Water Resources Research* 1 (1965): 283-286. Print.

Kutiel, P., H. Lavee, M. Segev, Y. Benyamini. "The effect of fire-induced surface heterogeneity on rainfall-runoff-erosion relationships in an eastern Mediterranean ecosystem, Israel." *Catena* 25 (1995): 77-87. Print.

Letey, J. "Causes and consequences of fire-induced soil water repellency." *Hydrological Processes* 15 (2001): 2867-2875. Print.

Martin, D.A., J.A. Moody. "Comparison of soil infiltration rates in burned and unburned mountainous watersheds." *Hydrological Processes* 15 (2001): 2893-2903. Print.

Mays, Larry W. "Water Resources Engineering." *John Wiley & Sons* (2001): 264. Print.

Moody, J.A., D.A. Martin. “Initial hydrologic and geomorphic response following a wildfire in the Colorado front range.” *Earth Surface Process and Landforms* 26 (2001): 1049-1070. Print.

Moody, J.A., D.A. Martin, S.L. Haire, D.A. Kinner. “Linking runoff response to burn severity after a wildfire.” *Hydrological Processes* 22 (2008): 2063-2074. Print.

Onset. “Barometric Compensation Assistant.” *White Paper Series* (2008): 1-4. Online.

---. “U2X Protective Housing – Housing-U2X.” *Onset Hobo Data Loggers* (2012). Online. 29 Oct. 2012.

Pechony, O., D.T. Shindel. “Driving forces of global wildfires over the past millennium and the forthcoming century.” *Proceedings of the National Academy of Sciences of the United States of America* 107.45 (2010): 19167-19170. Print.

Radeloff V.C., R.B. Hammer, S.I. Stewart, J.S. Fried, S.S. Holcomb, J.F. McKeefry. “The Wildland Urban Interface in the United States.” *Ecological Applications* 15 (2005): 799-805. Print.

Rulli, M.C., R. Rosso. “Hydrologic Response of Upland Catchments to Wildfires.” *Advances in Water Resources* 38.4 (1974): 652-657. Print.

Running, S.W. “Is Global Warming Causing More, Larger Wildfires?” *Science* 313 (2006): 927-928. Print.

Savage, S.M. “Mechanism of fire-induced water repellency in soil.” *Soil Science Society America Proceedings* 38 (1974): 652-657.

Scott, K.M. “Origin and sedimentology of 1969 debris flows near Glendora, California.” *United States Geological Survey Professor Paper* 750-C (1971): C242-C247. Print.

Shakesby, R.A. “Post-wildfire soil erosion in the Mediterranean: Review and future research directions.” *Earth-Science Reviews* 105 (2011): 71-100. Print.

Soil Survey Staff. “Web Soil Survey.” *National Resource Conservation Service.* Online. 03 February 2011.

Stewart, C., T. Kaplan-Henry. “Hydrology Specialist Report 2010 Bull Fire.” *Sequoia National Forest* (2010): 1-10. Online.

Terry, J.P., R.A. Shakesby. “Soil hydrophobicity effects on rainsplash: simulated rainfall and photographic evidence.” *Earth Surface Processes and Landforms* 18 (1993): 519-525. Print.

USFS RSAC. “BARC Data Bundle for the Bull Fire occurring on the Sequoia National Forest – 2010.” *USDA Forest Service.* 04 August 2010. Online. 25 September 2012.

Wells, W.G. II. “Some effects of brushfires on erosion processes in coastal Southern California.” *International Association of Hydrological Science* 132 (1981): 305-342. Print.

---. “The effects of fire on the generation of debris flows in southern California.” *Geological Society of America Reviews in Engineering Geology* 7 (1987): 105-114. Print.

Westerling, A.L., H.G. Hidalgo, D.R. Cayan, T.W. Swetnam. “Warming and Earlier Spring Increase Western U.S. Forest Wildfire Activity.” *Science* 313 (2006): 940-943. Print.

Wilson, C.J., J.W. Carey, P.C. Beeson, M.O. Gard, I.J. Lane. “A GIS-Based Hillslope Erosion and Sediment Delivery Model and Its Application to the Cerro Grande Burn Area.” *Hydrological Processes* 15 (2001): 2011-3023. Print.

Witt, S. “Burned Area Emergency Response, BAER.” *USDA Forest Service.* Watershed, Fish, Wildlife, Air & Rare Plants. 20 Jan 1999. Web. 09 Oct. 2012.

Zinke, P.J. “Forest interception studies in the United States.” *Forest Hydrology*, Sopper WE Lull HW (eds). Pergamon Press: New York, NY (1967): 137-161. Print.